

# **Broad Chain Length Specificity of the Alkane-Forming Enzymes NoCER1A and NoCER3A/B in *Nymphaea odorata***

This is a pre-copyedited, author-produced version of an article accepted for publication in *Plant and Cell Physiology* following peer review. The version of record will be available online at: <https://doi.org/10.1093/pcp/pcad168>.

## **Running head**

Water lily CER1/3 produces short chain alkanes

## **Corresponding author**

S. Ishiguro

Graduate School of Bio-agricultural Sciences,

Nagoya University, Nagoya 464-8601, Japan.

Telephone, +81-52-789-4097

Fax, +81+52-789-4107

Email, [guronyan@agr.nagoya-u.ac.jp](mailto:guronyan@agr.nagoya-u.ac.jp)

## **Subject area**

(4) Proteins, enzymes and metabolism

Black and white figure 1

Color figures 7

Table 0

Supplementary Figures 15

Supplementary Tables 3

# **Broad Chain Length Specificity of the Alkane-Forming Enzymes NoCER1A and NoCER3A/B in *Nymphaea odorata***

Hisae Kojima<sup>1,2</sup>, Kanta Yamamoto<sup>2</sup>, Takamasa Suzuki<sup>3</sup>, Yuri Hayakawa<sup>2</sup>, Tomoko Niwa<sup>2,†</sup>, Kenro Tokuhiro<sup>4</sup>, Satoshi Katahira<sup>4</sup>, Tetsuya Higashiyama<sup>5,6</sup>, and Sumie Ishiguro<sup>2,\*</sup>

<sup>1</sup>Technical Center, Nagoya University, Nagoya 464-8601, Japan

<sup>2</sup>Graduate School of Bio-agricultural Sciences, Nagoya University, Nagoya 464-8601, Japan

<sup>3</sup>College of Bioscience and Biotechnology, Chubu University, Kasugai 487-8501, Japan

<sup>4</sup>Toyota Central R&D Labs., Inc., Nagakute 480-1192, Japan

<sup>5</sup>Institute of Transformative Bio-Molecules (WPI-ITbM), Nagoya University, Nagoya 464-8601, Japan

<sup>6</sup>Graduate School of Science, The University of Tokyo, Tokyo 113-0033, Japan

<sup>†</sup>Current address: College of Bioscience and Biotechnology, Chubu University, Kasugai 487-8501, Japan.

\*Corresponding author: E-mail, [guronyan@agr.nagoya-u.ac.jp](mailto:guronyan@agr.nagoya-u.ac.jp)

## **Running head**

Water lily CER1/3 produce short chain alkanes

## ABSTRACT

Many terrestrial plants produce large quantities of alkanes for use in epicuticular wax and the pollen coat. However, their carbon chains must be long to be useful as fuel or as a petrochemical feedstock. Here, we focus on *Nymphaea odorata*, which produces relatively short alkanes in its anthers. We identified orthologs of the Arabidopsis alkane biosynthesis genes *AtCER1* and *AtCER3* in *N. odorata* and designated them *NoCER1A*, *NoCER3A*, and *NoCER3B*. Expression analysis of *NoCER1A* and *NoCER3A/B* in Arabidopsis *cer* mutants revealed that *N. odorata* enzymes cooperated with Arabidopsis enzymes and that NoCER1A produced shorter alkanes than AtCER1, regardless of which CER3 protein it interacted with. These results indicate that AtCER1 frequently uses a C30 substrate, whereas NoCER1A, NoCER3A/B, and AtCER3 react with a broad range of substrate chain lengths. The incorporation of shorter alkanes disturbed the formation of wax crystals required for water repellent activity in stems, suggesting that chain length specificity is important for surface cleaning. Moreover, cultured tobacco cells expressing *NoCER1A* and *NoCER3A/B* effectively produced C19–C23 alkanes, indicating that the introduction of the two enzymes is sufficient to produce alkanes. Taken together, our findings suggest that these *N. odorata* enzymes may be useful for the biological production of alkanes of specific lengths. Homology modeling revealed that CER1s and CER3s share a similar 3D structure that consists of N- and C-terminal domains, in which their predicted active sites are respectively located. We predicted the complex structure of both enzymes and found a cavity that connects their active sites.

## Keywords

Alkane-forming enzyme, *Arabidopsis thaliana*, carbon chain length, *Nymphaea odorata*, Tobacco BY-2 cell line, Wax crystals

## INTRODUCTION

Many land plants develop cuticles on the surface of their aboveground parts to protect the plants from environmental stresses including desiccation, rainfall, UV irradiation, and pathogen attack. The cuticle consists of two types of lipidic molecule: cutin and cuticular waxes. Cutin is a polyester mainly comprising hydroxy and epoxy 16 and 18 carbon (C16 and C18) fatty acids and glycerol, whereas cuticular waxes are mixtures of alkanes and other aliphatic compounds derived from very-long-chain (VLC, i.e., C21 and longer carbon chain) fatty acids (Bernard and Joubès 2013; Fich et al. 2016; Lee and Suh 2015). The latter are classified into intracuticular waxes, which are localized in the cutin layer, and epicuticular waxes, which form the outer coat of the cuticle (Aarts et al. 1995; Ariizumi et al. 2003; Chen et al. 2003; Fiebig et al. 2000; Haslam et al. 2015; Hülskamp et al. 1995; Ishiguro et al. 2010; Preuss et al. 1993). Epicuticular waxes often form small crystals that enhance the water repellency of plant surfaces (Neinhuis et al. 1992). Alkanes are also major constituents of the pollen coat, the outermost surface structure of pollen grains that is required for adhesion and interrecognition between pollen grains and stigmas (Hülskamp et al. 1995; Preuss et al. 1993).

In *Arabidopsis* (*Arabidopsis thaliana*), stem cuticular wax contains a mixture of alkanes and related molecules including aldehydes, alcohols, ketones, and fatty acids ranging C26–C31 in length (Jenks et al. 1995). The biosynthetic enzymes responsible for synthesizing these molecules are encoded by a subset of *ECERIFERUM* (*CER*) genes, and mutations in these genes cause wax-deficient phenotypes on the stem surface (Koornneef et al. 1989). To date, >25 *CER* and related genes in the *Arabidopsis* genome are thought to be involved in wax biosynthesis, transport, or regulation (Bernard and Joubès 2013; Lee and Suh 2015).

Alkane synthesis is initiated by the activation of C16 and C18 fatty acids to form acyl-coenzyme A (CoA) by a long-chain acyl-CoA synthetase (*lacs*) in the endoplasmic reticulum (ER), where the following process occurs. *CER8/LACSI* and related genes are thought to be involved in this process (Lü et al. 2009). *CER6*, also known as *CUT1*, encodes a  $\beta$ -ketoacyl-CoA synthase, a key component of the elongation system (Fiebig et al. 2000; Millar et al. 1999). Mutations in this gene cause the reduction of all wax monomers longer than C24, indicating that *CER6* is required for the elongation of fatty acyl-CoA beyond C24 (Millar et al. 1999). *CER6* alone can generate molecules up to C28 in length, but the co-expression of *CER2* or its related proteins with *CER6* can facilitate production of even longer fatty

acids (i.e., up to C34) (Haslam et al. 2015; Haslam et al. 2012). In rice, a similar interaction has been reported between WSL4 (a CER6 homolog) and OsCER2 (Wang et al. 2017). After elongation, VLC acyl-CoA enters either the alkane-forming or alcohol-forming pathway. In the alkane-forming pathway, VLC acyl-CoA is reduced to an aldehyde by *CER3* (also known as *FLP*, *WAX2*, or *YRE*)-encoded fatty acyl-CoA reductase, and this aldehyde is then converted to an alkane that is one carbon shorter in chain length via a *CER1*-encoded aldehyde decarbonylase (Aarts et al. 1995; Ariizumi et al. 2003; Bernard et al. 2012; Bourdenx et al. 2011; Chen et al. 2003; Kurata et al. 2003; Rowland et al. 2007). A similar two-step alkane-forming system also exists in cyanobacteria and insects, though the activity of the second enzyme is different. The byproduct of the *CER1* reaction is carbon monoxide, which is characteristic of plant alkane-forming enzymes. In contrast, cyanobacteria and animal enzymes generate formic acid and carbon dioxide, respectively (Cheesbrough and Kolattukudy 1984; Qiu et al. 2012; Warui et al. 2011).

*CER3* and *CER1* are localized in the ER membrane and are thought to form a complex *in vivo* (Aarts et al. 1995; Bernard et al. 2012; Millar et al. 1999). Although their enzyme activities are different, they are similar in amino acid sequence and probably originated in the common ancestor of the Viridiplantae (Chaudhary et al. 2021; Wang et al. 2019). *CER1* is presumably a non-heme iron enzyme that possesses a tripartite His cluster that is essential for its enzyme activity, whereas this motif is not necessary for functional *CER3* (Aarts et al. 1995; Bernard et al. 2012; Chen et al. 2003). Another conserved but functionally unknown *WAX2* domain is in their C-terminal regions. Bernard *et al.* (2012) showed that co-expression of *CER1* and *CER3* in a manipulated yeast strain producing VLC acyl-CoA resulted in production of C27–C31 alkanes, which matched the chain length distribution of alkanes in *CER1*-overexpressing *Arabidopsis* plants (Bourdenx et al. 2011). This finding indicated that *CER1* and *CER3* constitute a core complex of alkane synthesis enzymes that show strict carbon chain-length specificity for C28 and longer substrates. In contrast, *CER1-LIKE1*, a homolog of *CER1* that is predominantly expressed in flowers and siliques, involves the production of C25 and C27 alkanes (Greer et al. 2007; Pascal et al. 2019). It has been proposed that *CER1* and *CER1-LIKE1* form distinct complexes with *CER3* that work in a complementary manner in wax synthesis in flowers. In rice, three *CER1* homologs (OsGL1-4/OsCER1, OsGL1-5/WDA1, and OsGL1-6) and three *CER3* homologs (OsGL1-1/WSL2, OsGL1-2, and OsGL1-3) coordinate during alkane production (Islam et al. 2009; Jung et al. 2006; Mao et al. 2012; Ni et al. 2018; Qin et al. 2011; Zhou et al. 2013; Zhou et al. 2015).

In some plant families, including the Brassicaceae, secondary alcohols and ketones are generated by midchain alkane hydroxylase, which facilitates hydroxylation and oxidation at the central carbon of alkanes (Greer et al. 2007). Most alkanes, secondary alcohols, and ketones generated by this pathway are odd-numbered carbon molecules, since the terminal carbon atoms of VLC acyl precursors, which usually have an even carbon number, are removed during the CER1-catalyzed decarbonylation step. In the alcohol-forming pathway, VLC acyl-CoA is presumed to be converted to a potential intermediate aldehyde then changed to a primary alcohol by a single reducing enzyme, CER4 (Rowland et al. 2007). This alcohol is subsequently used for ester formation, predominantly with C16 fatty acids (Lai et al. 2007).

Since alkanes are major components of fuels used by internal-combustion engines, efforts have been made to develop biological production of alkanes by microorganisms. For example, metabolically modified *Escherichia coli* harboring acyl-acyl carrier protein reductases and aldehyde-deformylating oxygenases from cyanobacteria have been demonstrated to produce C13–C17 alkanes and alkenes, which are appropriate for diesel fuel (Schirmer et al. 2010). Expression of *Clostridium acetobutylicum* fatty acyl-CoA reductase and Arabidopsis CER1 with other enzymes in *E. coli* resulted in the production of relatively short C9–C14 alkanes and alkenes (Choi and Lee 2013). Similar approaches have been developed by eukaryotic organisms such as yeast and algae using enzymes derived from various organisms. However, neither CER1 nor CER3 have yet been successfully used in any of these systems (Foo et al. 2017; Hu et al. 2019; Kang et al. 2017; Li et al. 2020; Monteiro et al. 2022; Yunus et al. 2018). One possible reason for their omission may be the specificity of Arabidopsis proteins for C28 and longer substrates (Bernard et al. 2012).

The epidermal cells of land plants preferentially produce non-volatile VLC alkanes, which are used as structural components and surface protectant. However, some plants also produce volatile alkanes as odors in pollen and flowers (Bertoli et al. 2011; Mukherjee et al. 2013; Tsai 2019). These volatile alkanes are relatively short and are suitable for biofuels. Moreover, it is expected that plants may have alkane synthetic enzymes that are even more suitable for biofuel production than those found in yeast and algae, since in plants these enzymes are localized to the ER, the central place of lipid metabolism in eukaryotic cells (Garay et al. 2014; Henry et al. 2012). To determine whether this is the case, we have analyzed the pollen coat lipid composition of 290 plant species and found that the pollen coat of a water lily (*Nymphaea odorata*) contained shorter-chain alkanes (i.e., alkanes as small as C15). In this paper, we

identified and characterized the CER1 and CER3 homologs of *N. odorata*, and found that they are able to produce shorter VLC alkanes in Arabidopsis plants and cultured tobacco cells.

## RESULTS

### *N. odorata* Accumulates Shorter VLC Alkanes in its Pollen Coat than Arabidopsis

The pollen coat was first extracted from pollen grains harvested from the fully opened flowers of a temperate water lily, *N. odorata*. Then the sample was analyzed using a gas chromatograph-mass spectrometer (GC-MS) equipped with a DB-1 nonpolar capillary column. This result showed that the *N. odorata* pollen coat included normal alkanes with carbon chain lengths ranging C15–C29, of which C19, C21, and C23 molecules were the most abundant (Fig. 1A). Small amounts of C16 and C18 saturated fatty acids and some terpenoids were also detected. In Arabidopsis (*Arabidopsis thaliana* accession Columbia-0 (Col-0)), the pollen coat mainly consisted of normal and branched alkanes (Busta and Jetter 2017), of which the normal C29 alkane was the most abundant (Fig. 1B). Moreover, we also detected 15-nonacosanol and nonacosan-15-one, which are oxidized derivatives of normal C29 alkanes (Greer *et al.*, 2007). The carbon chain lengths of Arabidopsis pollen coat components were distributed from C27 to C31, which is the most common range for angiosperms. Taken together, these results indicate that *N. odorata* can synthesize relatively short chain alkanes for pollen coat production.

### Identification and CDS Cloning of *CER1* and *CER3* Homologs in *N. odorata*

Since the chain length range of pollen coat alkanes depends on the characteristics of alkane synthetic enzymes, we expect that the enzymes present in *N. odorata* can produce shorter-chain alkanes. To test this possibility, we attempted to identify the homologs of

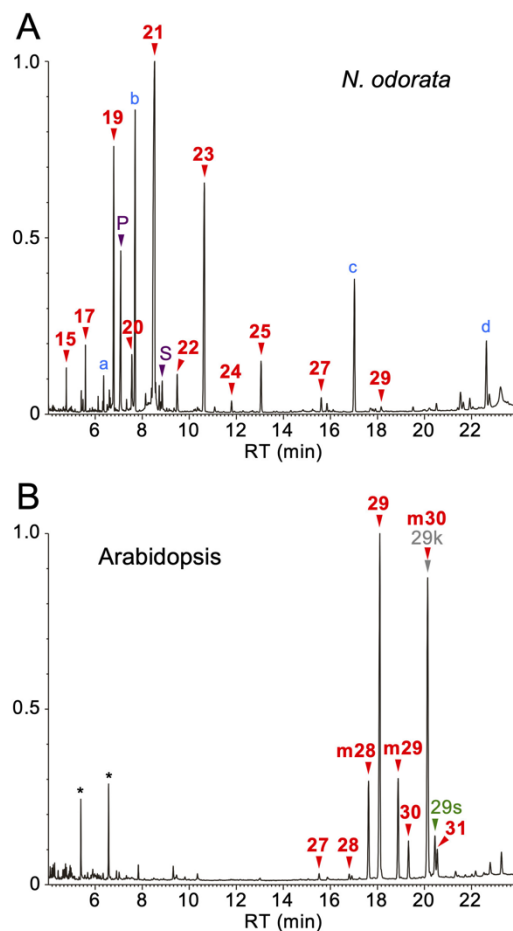


**Figure 1**  
**Total ion current chromatogram of the GC-MS analysis of pollen coat lipids.**

(A) *N. odorata*. (B) Arabidopsis. Arrowheads indicate the peaks of aliphatic compounds of the indicated carbon-chain length. Red, alkanes (numbers only); purple, fatty acids (P, palmitic acid; S, stearic acid); gray, ketones (labeled by 'k'); green, secondary alcohols (labeled by 's'). Alkanes labeled by 'm' are branched 2-methylalkanes. The peaks of 2-methyltriacontane and nonacosan-15-one are overlapping. a to d in panel (A) are terpenoids (a, phytol; b, geranylinalool; c, squalene; d,  $\beta$ -sitosterol). Asterisks in (B) are artifacts due to column contamination. RT, retention time. The vertical axis shows the relative intensity when the maximum peak is set as 1.0.

*Arabidopsis CER1* (hereafter *AtCER1*) and *AtCER3* genes in *N. odorata*. An RNA sample isolated from young *N. odorata* anthers was reverse transcribed and analyzed by paired-end tag sequencing on a next generation sequencing platform. A BLAST search with *AtCER1* as the query sequence identified a sequence contig, named *CER1* homolog A, which matched the full-length protein coding sequence (CDS) of *AtCER1*. Similarly, we also identified two contigs homologous to *AtCER3* CDS throughout their entire sequence (*CER3* homologs A and B). All three contigs contained SNPs that accounted for 2% of the total CDS nucleotides. Of these SNPs, one-third to one-half were nonsynonymous, and are presumably attributed to the multiploidy of this species (Supplementary Table S1) (Pellicer et al. 2013).

We prepared PCR primers for amplifying the full-length CDS of each of these genes. We obtained three CDS clones, designated *NoCER1A*, *NoCER3A*, and *NoCER3B*. The entire amino-acid sequence of *NoCER1A* was compared to those of *AtCER1* and its close homologs in alfalfa, tomato, rice, and *Amborella trichopoda*, a species that, like water lily, belongs to the basal angiosperms (Supplementary Fig. S1 and Supplementary Table S2). Although the whole-gene sequences of the *CER1* proteins were only somewhat similar, tripartite His clusters, which have been shown to be indispensable for the enzyme activity of *AtCER1* (Bernard et al. 2012; Chen et al. 2003), were highly conserved in the N-terminal halves of the proteins sequences. Moreover, alignment of the whole *NoCER3A* and *NoCER3B* sequences with *AtCER3* and its close homologs revealed that their C-terminal halves, including the WAX2 domain, were highly conserved (Supplementary Fig. S2). The *NoCER1A* and *CER1* homologs also contained the WAX2 domain in their C-terminus, though this region showed less homology (Supplementary Fig. S1). We performed a phylogenetic analysis on all *CER1* and *CER3* homologs using whole genome sequence data for each of these plant species as well as sequence data for a predicted common ancestral protein, *OICER1/3*, from *Osterococcus lucimarinus* (Chaudhary et al. 2021). Our data suggest that in *CER1* homologs, the *NoCER1A* and *A. trichopoda* proteins first branched out from the others, which is consistent with the position of water lilies in angiosperm evolution (Fig. 2). Similarly, the *NoCER3A*, *NoCER3B* and *A. trichopoda* proteins also branched out earlier than others (Fig. 2). These results suggest that *NoCER1* and *NoCER3* belong to the *CER1* and *CER3* gene families, respectively, but they are structurally different from other angiosperm homologs. The sequence identities among *CER1* homologs from different species (i.e., ~50%–60%) were relatively lower than those among *CER3* homologs (i.e., ~60%–70%) (Supplementary Fig. S3). This pattern was particularly striking among *CER1* homologs in *N. odorata*, *A. trichopoda*, *Arabidopsis*, and rice, which is consistent with

the long branch lengths found on the dendrogram (Fig. 2). Structural diversity was also observed among the intraspecific CER1 homologs in these species (Supplementary Fig. S3).

We also carried out RT-PCR using degenerate primers designed according to the sequences of 26 *CER1* and 15 *CER3* homologs found in public databases (Supplementary Figs. S1 and S2 and Supplementary Table S3). By use of DNA reverse transcribed from young anther RNA, we amplified a *CER1*-related sequence corresponding to *NoCER1A* and two *CER3*-related sequences that match *NoCER3A* and *NoCER3B*. This result supported that these genes are actively expressing *CER1* and *CER3* homologs in the anthers of *N. odorata*.

In a recently published reference genome for tropical water lily, *Nymphaea colorata*, two *CER3* homologs corresponding to *NoCER3A* and *NoCER3B* and two tandem genes that were both similar to *NoCER1A* were identified (Supplementary Fig. S4) (Zhang et al. 2020). Hence, we concluded that we cloned the orthologs of *AtCER1* and *AtCER3* in *N. odorata*, and that they are actively transcribed in anthers.

### Co-expression of *NoCER1A* and *NoCER3A/B* Restored Alkane Biosynthesis in *Arabidopsis cer1 cer3* Double Mutants

In order to evaluate the enzyme activities of *NoCER1A*, *NoCER3A*, and *NoCER3B*, we designed a complementation experiment using *Arabidopsis cer1 cer3* double mutants. The mutant alleles used in

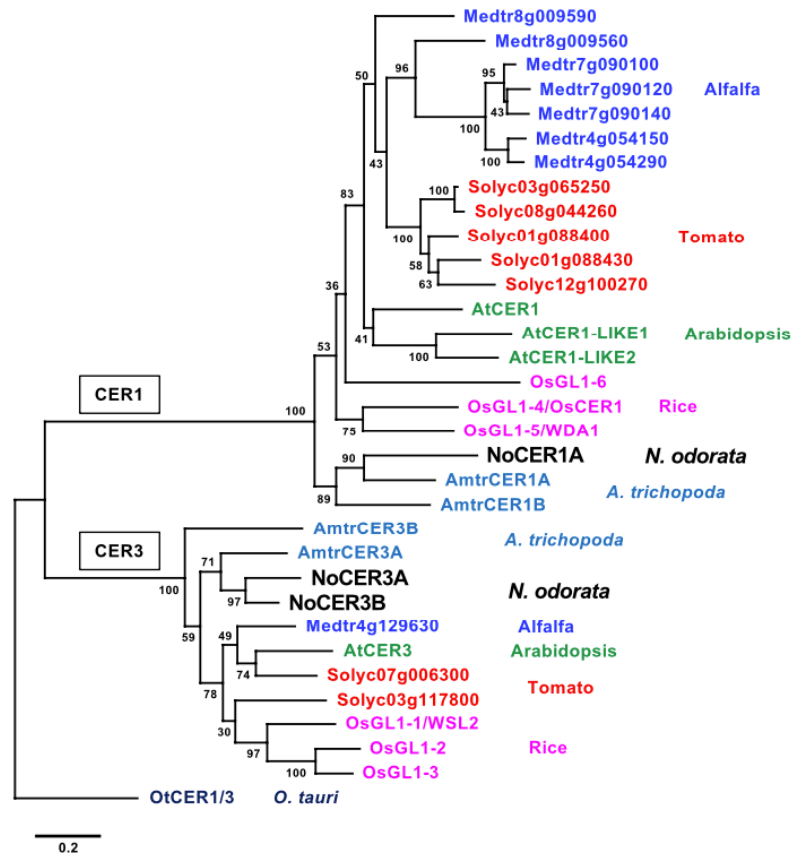


**Figure 2**  
**Structural relationships among CER1 and CER3 proteins in *N. odorata* and representative angiosperms.**

Maximum likelihood phylogenetic tree of *NoCER1A*, *NoCER3A*, *NoCER3B*, and their homologous proteins in tomato, alfalfa, Arabidopsis, rice, and *A. trichopoda*. A predicted common homolog in *O. tauri* is added as an outgroup. Proteins are color coded according to species. Bootstrap support values from 1000 replicates are indicated. The bar represents 0.2 substitutions per site.

this study were *cer1-1* (SALK\_008544) and *cer3-9* (GABI\_177D09). Both are virtually null alleles disrupted by T-DNA insertions into the tenth exon and fourth intron of the respective genes (Supplementary Figs. S5 and S6) (Bourdenx et al. 2011; Xu et al. 2019). We connected the *NoCERIA* CDS with the *AtCER1* promoter (*ProAt1*; -1208 to -1; the A of the ATG start codon was set to +1). For CER3, we noted that previous reports found that the exon 1 and intron 1 of *AtCER3* are important for efficient promoter activity (Kurata et al. 2003). Hence, we connected the CDS of *NoCER3A* and *NoCER3B* to an extended version of the *AtCER3* promoter (*ProAt3i*; -1748 to +144), which contained a 17-amino-acid N-terminal sequence of *AtCER3* in exon 1 as well as all of intron 1 (Supplementary Fig. S8). The modified forms of *NoCER3A* and *NoCER3B* contained five and six amino-acid substitutions relative to the original *NoCER3A* and *NoCER3B* sequences, respectively (Supplementary Fig. S8). These genes were introduced into the double mutants by *Agrobacterium*-mediated transformation. Once grown, we extracted and analyzed the stem cuticular wax of the transgenic plants instead of pollen coat lipids, because the former is more abundant in *Arabidopsis* than the latter.

A GC-MS analysis of the wild-type *Arabidopsis* (WT) revealed that the stem cuticular wax contained a considerable amount of unbranched VLC alkanes of odd-number chain lengths (i.e., C27, C29, and C31); 15-nonacosanol (C29-15-alcohol) and 15-nonacosanone (C29-15-ketone), both of which are derived from C29 alkane; C26, C28, and C30 VLC aldehydes; and C26 and C28 primary alcohols (Fig. 3A). Of these products, C29 alkane and C29-15-ketone were the most abundant. This result was consistent with previous reports (Goodwin et al. 2005; Jenks et al. 1996). Small amounts of alkyl esters consisting of C12–C18 fatty acids and C24–C30 alcohols were detected by a GC-MS analysis performed with an increased sample amount and an extended retention time (Supplementary Fig. S9). In this experiment, minor components such as C24 and C30 alcohols, even-numbered alkanes, and odd-numbered aldehydes were also identified (Supplementary Fig. S9). In contrast, alkanes and the alkane derivatives were rarely detected on the surface of *cer1 cer3* stems, whereas small peaks of aldehydes and primary alcohols were readily observed (Fig. 3B).

Transgenic *cer1 cer3* plants in the T1 generation carrying *ProAt1-NoCERIA* and *ProAt3i-NoCER3A* genes produced a considerable amount of odd-numbered alkanes ranging C23–C29 in length, of which C29 was the most abundant (Fig. 3C). Similar results were obtained when *ProAt1-NoCERIA* and *ProAt3i-NoCER3B* were expressed (Fig. 3D). The alkane levels of these transformants were much higher than those of parental *cer1 cer3* double mutants and were comparable to those of WT plants (Fig.

3F). We used triterpenoid  $\beta$ -amyryn, a major constituent of intracuticular wax (Buschhaus and Jetter 2012), as an endogenous internal standard for alkane quantification instead of adding any exogenous internal standards, which might be included in the sample. To evaluate the enzyme preference for shorter molecules, we calculated the ratio of C28 and shorter alkanes against total alkane content. The values for *NoCER1A* and *NoCER3A/B* expressing plants reached ~30%, whereas that of WT was less than 0.1% (Fig. 3F). As a control experiment, transgenic *cer1 cer3* plants containing *ProAt1-AtCER1* and *ProAt3i-AtCER3* genes produced stem wax in an amount and with a composition that was comparable to the WT (Fig. 3E and F and Supplementary Fig. S8). These results indicate that water lily enzymes had greater alkane synthetic activity and used broader chain length acyl-CoA substrates relative to *Arabidopsis* enzymes.

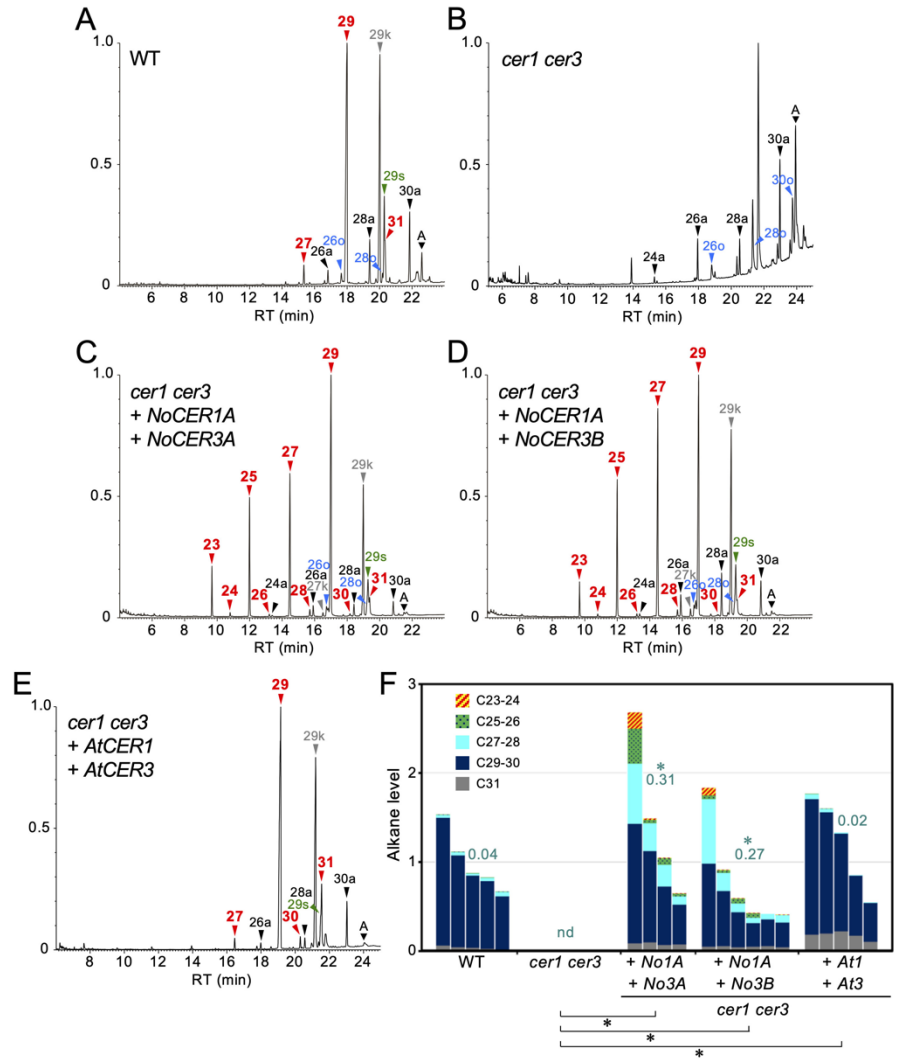


**Figure 3**  
**Restored alkane production in the stems of *Arabidopsis cer1 cer3* plants expressing both *NoCER1A* and *NoCER3A/B*.**

(A–E) Total ion current chromatogram of the GC-MS analysis. Typical results of the WT (A), *cer1 cer3* double mutants (B), *cer1 cer3* containing *ProAt1-NoCER1A* and *ProAt3i-NoCER3A* (C), *cer1 cer3* containing *ProAt1-NoCER1A* and *ProAt3i-NoCER3B* (D), and *cer1 cer3* containing *ProAt1-AtCER1* and *ProAt3i-AtCER3* (E) are shown. The vertical axis shows the relative intensity when the maximum peak is set as 1.0. Colored arrowheads indicate the peaks of compounds of the indicated carbon-chain length. Red, alkanes (numbers only); black, aldehydes (labeled by 'a'); gray, ketones (labeled by 'k'); green, secondary alcohols (labeled by 's'); blue, primary alcohols (labeled by 'o'). A,  $\beta$ -amyryn, an internal standard for quantification. Peaks with no labels are unidentified compounds. (F) Comparison of alkane levels shown as relative values compared to the average of the WT. Bars represent individual WT, *cer1 cer3*, and independent T1 transformant plants. The ranges of carbon-chain lengths are shown in different colors. Dark green values represent the average ratios of C28 and shorter alkanes against total alkanes. Asterisks indicate statistically significant differences of total alkane amount from *cer1 cer3* (black) and of shorter alkane ratio from WT (dark green), respectively (Steel's test,  $P < 0.05$ ). nd, not determined due to no detection of alkanes.

To confirm these results, we used T2 transformants of the representative lines to determine the levels and carbon chain length compositions of the major aliphatic components present in stem wax. We used six to eight T2 plants of each line and measured the quantities of the query compounds in a specified surface area. Measurements were normalized to an exogenously added C15 alkane standard. To estimate the amounts of aldehydes and alcohols, we determined 1.0 and 0.19 as relative response factors for these compound classes, respectively. As reported previously, *cer1* plants produced only trace levels of alkanes, indicating that CER1 activity is almost essential for alkane synthesis in stems (Supplementary Fig. S10A). This mutant accumulated C30 aldehyde approximately twice as much as the WT, although the levels of increased aldehydes were lower than the levels of decreased alkanes (Supplementary Fig. S10B). Moreover, alcohol production was also inhibited in the mutant (Supplementary Fig. S10C). These results suggest that the activity of CER3 was inhibited by the lack of CER1 protein or by the accumulation of the potentially toxic C30 aldehyde. In contrast, *cer3* mutant produced a low but still considerable amount of alkanes (Supplementary Fig. S10A). In this mutant, aldehydes and C26 and C28 alcohol production decreased, whereas C30 alcohol production increased (Supplementary Fig. S10B and C). Because the *cer3* allele used in this study was virtually a null allele, our results suggest that a fatty acid reductase other than CER3 contributed to C30 aldehyde formation, which was efficiently converted to C29 alkane and C30 alcohol. In *cer1 cer3* double mutants, the combined effects of both mutations were apparent. Alkanes and aldehyde levels were markedly decreased, whereas the abundance of C30 alcohol slightly increased, though its amount was much lower than the level of C29 alkane measured in the WT (Supplementary Figs. S10A–C). The alkane levels of T2 transformants co-expressing the *ProAt1-NoCER1A* and *ProAt3i-NoCER3A* (or *ProAt3i-NoCER3B*) genes in the *cer1 cer3* double mutant background were lower than in parental T1 transformants, probably due to reductions in gene expression. Nevertheless, the preference of the enzymes for shorter substrates was clearly demonstrated; this is evident from the ratios of C28 and shorter alkanes to total alkanes in the transformants being higher than those of the WT (i.e., 0.24, 0.19, and 0.04 for NoCER1A + NoCER3A plants, NoCER1A + NoCER3B plants, and WT plants, respectively) (Supplementary Fig. S10A). Aldehyde and alcohol levels were moderate in the transformants (Supplementary Fig. S10B and C).

### **NoCER1 and NoCER3 Functionally Interact with Arabidopsis CER3 and CER1 Enzymes**

Previous studies have shown that AtCER1 and AtCER3 interact with each other to form an enzymatic

complex (Bernard et al. 2012). To examine whether *N. odorata* enzymes could work together with Arabidopsis enzymes, *NoCERIA* and *NoCER3A/B* genes were separately introduced into Arabidopsis *cer1* and *cer3* mutants, respectively, and their alkane synthetic activities were assayed. In this experiment, the *AtCER1* promoter was used for expressing the intact CDSs of both *NoCERIA* and *NoCER3A/B* genes (Supplementary Fig. S8). The expression of *NoCERIA* restored alkane synthesis activity in *cer1*, but the alkane chain length was shortened to C23, resembling the results of the *NoCER1/NoCER3*

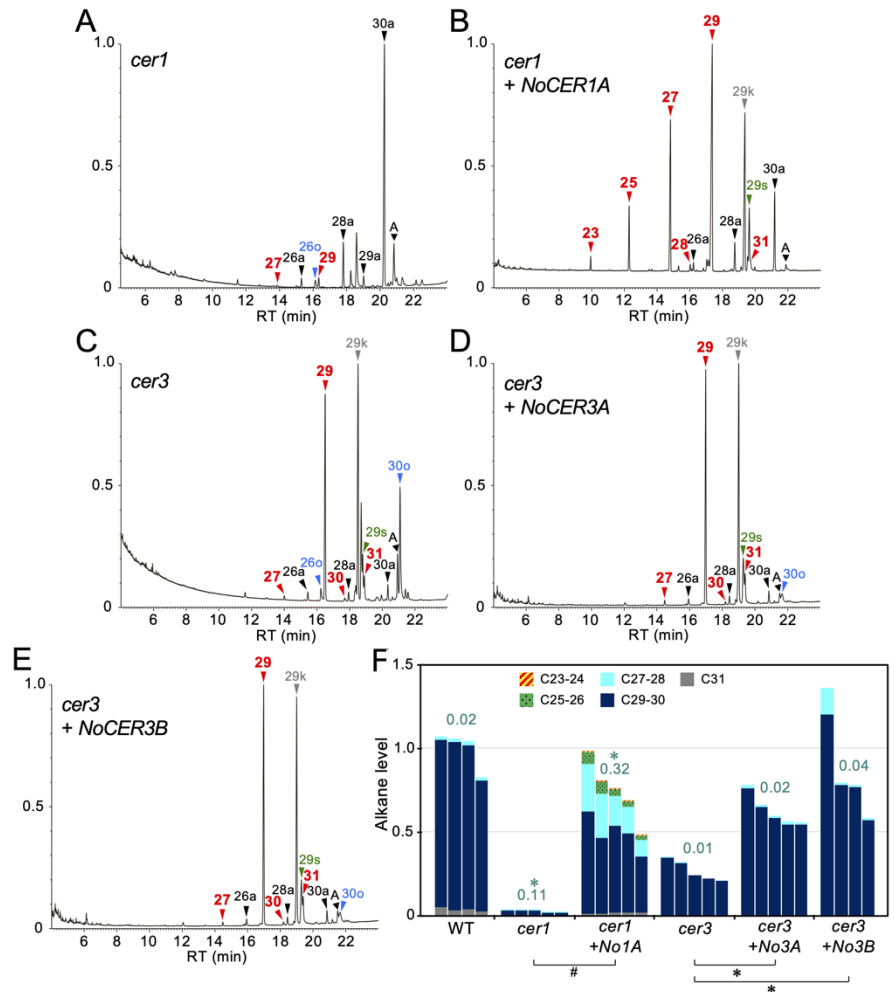


**Figure 4**  
**Contribution of NoCERIA and NoCER3A/B to the chain length specificity of alkanes produced in Arabidopsis stems.**

(A–E) Total ion current chromatogram of GC-MS analysis. Typical results of *cer1* (A), *cer1* containing *ProAt1-NoCERIA* (B), *cer3* (C), *cer3* containing *ProAt1-NoCER3A* (D), and *cer3* containing *ProAt1-NoCER3B* (E) are shown. (F) Quantification of alkane levels. Statistically significant differences of shorter alkane ratio from WT (dark green \*, Steel's test,  $P < 0.05$ ), of total alkane level from *cer1* (#, U-test,  $P < 0.05$ ), and of total alkane levels from *cer3* (black \*, Steel's test,  $P < 0.05$ ) are indicated. Other details are explained in Figure 3 legend.

coexpression in the *cer1 cer3* double mutants (Fig. 4B and F). This indicated that NoCER1A had CER1 activity and worked together with AtCER3 (or subsidiary aldehyde-forming enzymes detected in the *cer3* mutant) to produce various alkane chain lengths. Transgenic *cer3* plants expressing *NoCER3A* or *NoCER3B* restored the levels of alkane production, and the lipid composition of their stem wax was similar to that of the WT (Fig. 4D–F). This indicated that NoCER3A/B had CER3 activity and worked together with AtCER1 but did not affect the chain length of the alkane product. In summary, our data showed that the CER1 and CER3 enzymes in *N. odorata* and Arabidopsis functionally interacted with each other, and CER1, but not CER3, determined chain length specificity. In other words, NoCER1A

combined with all examined CER3 generates various substrate chain lengths, whereas AtCER1 shows strict chain length specificity for C27–C31 substrates.

### NoCER1A Produces Shorter-Chain Alkanes in the *cer6* Mutant

Whereas *N. odorata* effectively produced C19–C23 alkanes in anthers, the transgenic *Arabidopsis* described above produced negligible amounts of these short alkanes. We assumed that acyl-CoA substrates of C24 and shorter were less abundant in *Arabidopsis* stems, since these have a strong fatty acid elongase activity. Thus, we employed the *cer6* mutant, which lacks a fatty acid elongase required to produce C24–C28 acyl-CoAs (Haslam and Kunst 2013). We chose an allele in the Col-0 background, GABI\_804G08, which has a T-DNA insertion in the first intron of the *CER6* gene, and named it *cer6-4* (Supplementary Fig. S5). Although this was not a null allele, we confirmed that the

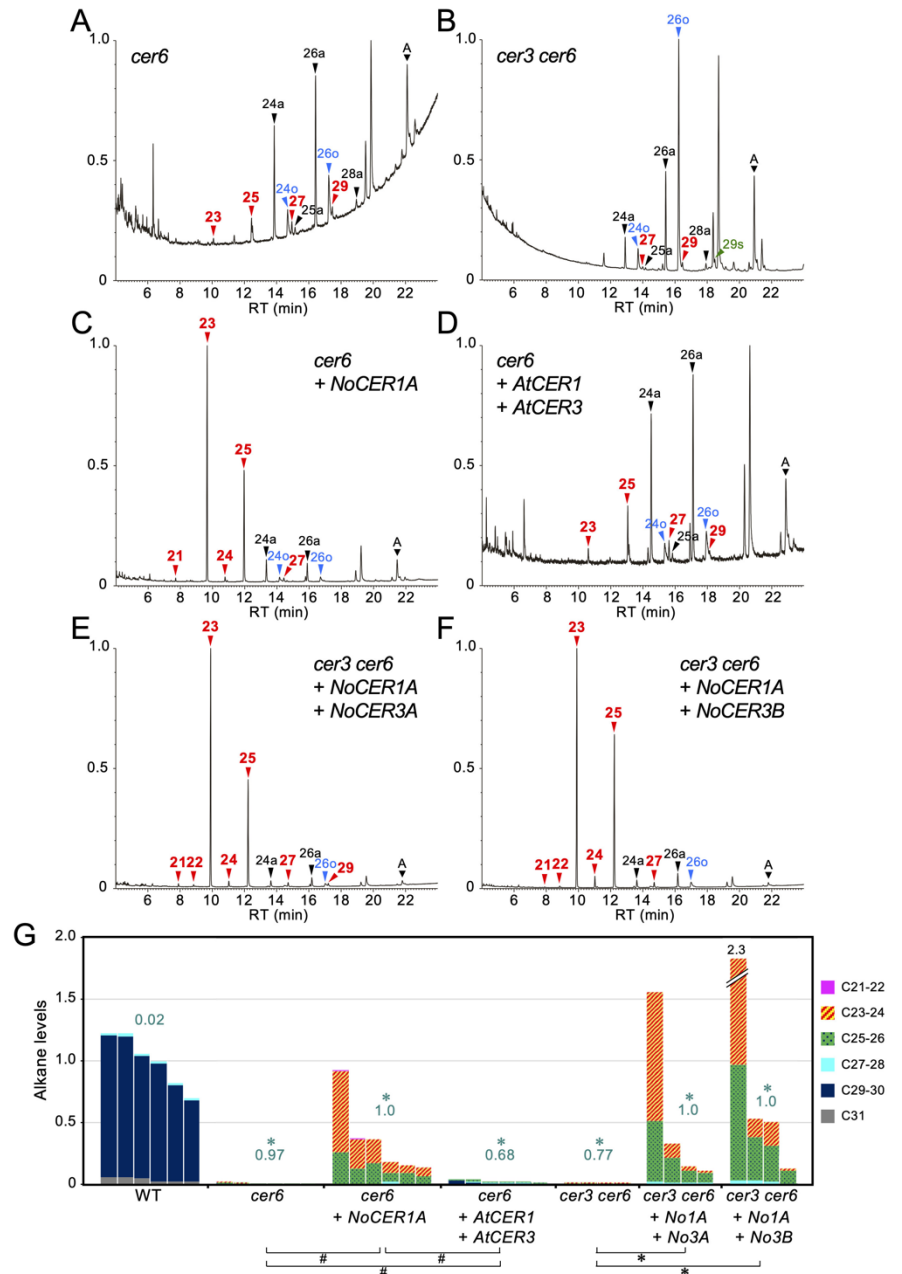


**Figure 5**  
**Production of short VLC alkanes in *cer6* and *cer3 cer6* mutants expressing *N. odorata* genes.**

(A–F) Total ion current chromatogram of GC-MS analysis. Typical results of *cer6* (A), *cer6* containing *ProAt1-NoCER1A* (B), *cer6* containing *ProAt1-AtCER1* and *ProAt3-AtCER3* (C), *cer3 cer6* (D), *cer3 cer6* containing *ProAt1-NoCER1A* and *ProAt1-NoCER3A* (E), and *cer3 cer6* containing *ProAt1-NoCER1A* and *ProAt1-NoCER3B* (F) are shown. (G) Quantification of alkane levels. Statistically significant differences of shorter alkane ratio from WT are indicated (dark green \*, Steel’s test,  $P < 0.05$ ). Relationships of total alkane levels with a statistically significant difference are shown (Steel’s test [\*] and Steel-Dwass test [#],  $P < 0.05$ ). Other details are explained in Figure 3 legend.

level of CER6 mRNA in the mutant was <1% of that in the WT (Supplementary Fig. S7). Consistent with previous reports (Fiebig et al. 2000; Goodwin et al. 2005), the *cer6* mutant produced only small amounts of C23–C29 alkanes but also produced relatively large amounts of C24 and C26 aldehydes and alcohols (Fig. 5A and G and Supplementary Fig. S10). When we introduced the *ProAt1-NoCER1A* gene into *cer6*, the transformants produced remarkable amounts of C23 and C25 alkanes as well as low but detectable levels of newly observed C21 and C24 alkanes. These data indicate that NoCER1A can produce short VLC alkanes in combination with endogenous Arabidopsis fatty acyl reductases (Fig. 5C and G). In a control experiment, the expression of *ProAt1-AtCER1* together with *ProAt3-AtCER3* in the *cer6* mutant, in which the endogenous *AtCER1* and *AtCER3* genes were functional, did not show altered wax composition, although alkane levels were slightly increased (Fig. 5D and G).

Next, we expressed both *ProAt1-NoCER1A* and *ProAt1-NoCER3A* (or *ProAt1-NoCER3B*) genes in *cer3 cer6* double mutants. These transformants predominantly produced C23 and C25 alkanes, and the wax composition was similar to that of the *ProAt1-NoCER1A* transformants in the *cer6* background (Fig. 5E–G). Similar characteristics were observed in T2 progeny of the *ProAt1-NoCER1A* and *ProAt1-NoCER3B* transformants, although their alkane levels were lower than those of the parental T1 plants (Supplementary Fig. S10). Based on these results, we hypothesized that NoCER1 worked together with NoCER3A, NoCER3B, and AtCER3 to produce short VLC alkanes in Arabidopsis. However, wax quantification revealed that the levels of C24 and C26 aldehydes did not significantly differ between the *cer6* and *cer3 cer6* double mutants; moreover, more C26 alcohol was produced in the latter (Supplementary Fig. S10). This result indicated that C24 and C26 acyl-CoAs accumulated by defective CER6 elongase were efficiently converted to aldehydes and alcohols and that AtCER3 was not primarily responsible for this reaction. Accordingly, it cannot be ruled out that alternate endogenous reductase activity in Arabidopsis (i.e., other than AtCER3) may contribute to shorter alkane production in combination with NoCER1. Hence, we decided to use cultured tobacco cells to examine the contribution of NoCER3 to short VLC alkane production.

### **Coexpression of *NoCER1A* and Any of the *CER3* Genes is Sufficient for Alkane Production in Cultured Tobacco Cells**

Untransformed calli of BY-2 tobacco cultured cells grown on agar plates did not produce detectable amounts of wax components but accumulated abundant C16 and C18 fatty acids (Fig. 6A and G).

Introduction of *NoCER1A* driven by a cauliflower mosaic virus 35S promoter (*Pro35S*) did not by itself cause the production of any alkanes and aldehydes; the result confirmed that *NoCER1A* alone could not produce these compounds and that the cells lack endogenous reductase activities that work together with *NoCER1A* (Fig. 6B and G). Next, to test whether the coexpression of *NoCER1A* and *NoCER3A/B* is sufficient to synthesize alkanes, we introduced both *Pro35S-NoCER1A* and *Pro35S-NoCER3A* into the BY-2 cells. The transformants produced alkanes between C17 and C25 in length, and C19, C21, and C23 species were the most abundant (Fig. 6C and G). The introduction of the *Pro35S-NoCER1A* and *Pro35S-NoCER3B* pair provided a similar result, except that the abundance of the C17 and C19 alkanes decreased (Fig. 6D and G). The alkane levels in the transformants reached 43–53  $\mu\text{g}$  per g fresh cell weight (Supplementary Fig. S11), which was calculated to be 1.0–1.3 mg per g dry cell weight. A control experiment introducing *Pro35S-AtCER1* and *Pro35S-AtCER3* did not produce any alkanes in BY-2 cells

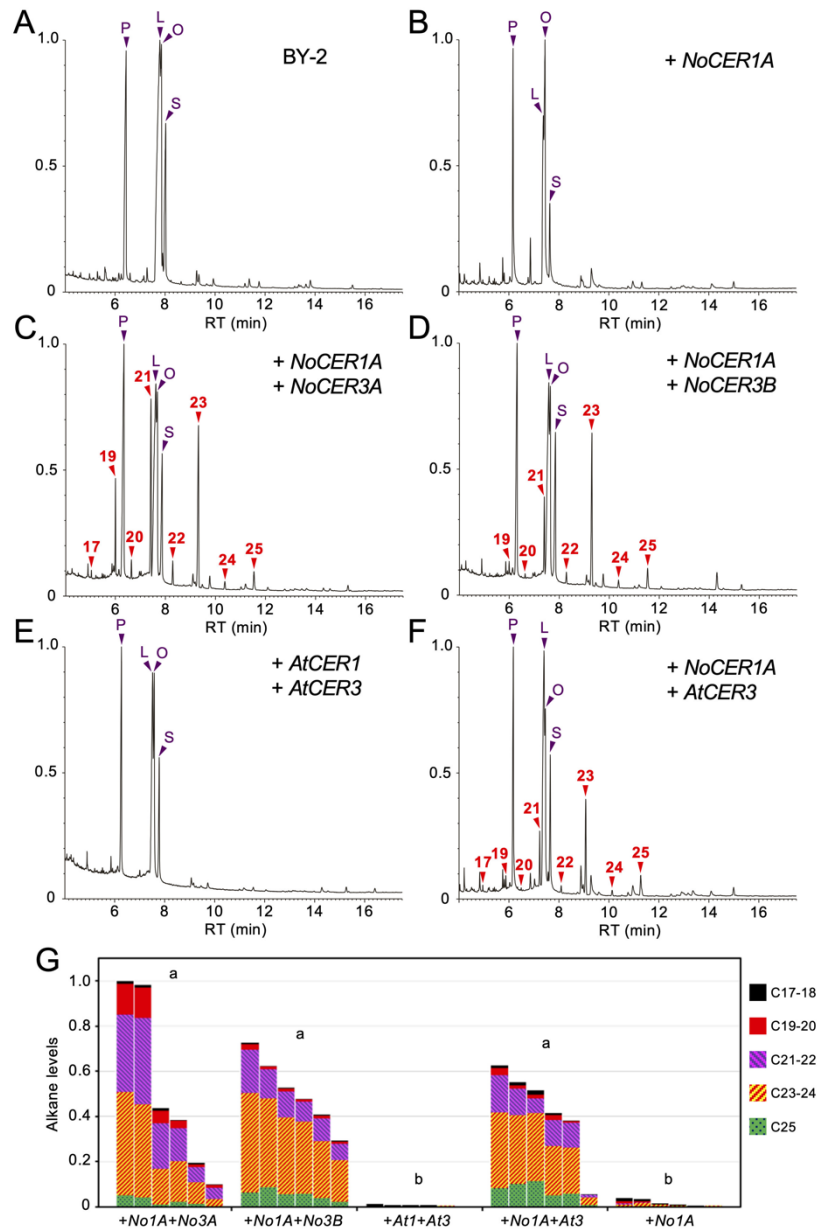


**Figure 6**  
**Alkane production in tobacco BY-2 cells expressing *NoCER1A* and various *CER3* genes.**

(A–F) Total ion current chromatogram of the GC-MS analysis. Typical results of a non-transformed BY-2 callus (A) and BY-2 calli containing *Pro35S-NoCER1A* alone (B), *Pro35S-NoCER1A* and *Pro35S-NoCER3A* (C), *Pro35S-NoCER1A* and *Pro35S-NoCER3B* (D), *Pro35S-AtCER1* and *Pro35S-AtCER3* (E), and *Pro35S-NoCER1A* and *Pro35S-AtCER3* (F) are shown. The vertical axis shows the relative intensity when the maximum peak is set as 1.0. Alkane peaks are labeled with red numbers indicating carbon-chain length. P, palmitic acid; L, linoleic acid; O, oleic acid; S, stearic acid. (G) Total alkane levels in six independently obtained transformants expressing indicated genes. Ranges of carbon-chain lengths are shown in different colors. Levels are shown in arbitrary units. Significant differences determined by Tukey’s test ( $P < 0.05$ ) are indicated by letters above the bars.

(Fig. 6E and G). Nevertheless, cells expressing *NoCER1A* and *AtCER3* produced similar sets of alkanes, indicating that *NoCER3* can be replaced by *AtCER3* (Fig. 6F and G). Taken together, these results indicate that the coexpression of *NoCER1A* and any one of *NoCER3A*, *NoCER3B*, or *AtCER3* was sufficient to produce alkanes in BY-2 cells. *NoCER1A* and *CER3s* catalyze reactions for a broad range of chain lengths of acyl substrates, whereas *AtCER1* has strict substrate specificity for C28–C32 molecules that are efficiently produced in certain cells such as the Arabidopsis epidermis.

### Alkane Chain Length is Important for the Formation of Wax Crystals Required for Self-Cleaning

Scanning electron microscopy revealed that many wax crystals were deposited on the stem surface of WT Arabidopsis plants (Fig. 7A), while the waxless *cer1* mutant showed no such crystal formation as well as male sterility caused by defective pollen coat formation (Fig. 7B and E). Transgenic *cer1* plants

containing *ProAt1-NoCER1A* showed a restored ability to produce C23–C29 alkanes in stems and to set self-pollinated seed, but irregular scales instead of wax crystals were formed on the stems (Figs. 4B, 7C, and 7F). The amount of nonalkane wax components did not significantly differ between the *ProAt1-NoCER1A* and WT plants (Supplementary Fig. S12), indicating that mixed shorter alkanes inhibited the formation of a crystalline structure. Wax crystals are thought to be involved in a self-cleaning process called the lotus effect, by which water is repelled by the crystalline microstructure and forms droplets; these droplets wash away pollutants and pathogen spores deposited on the plant surface. Here,

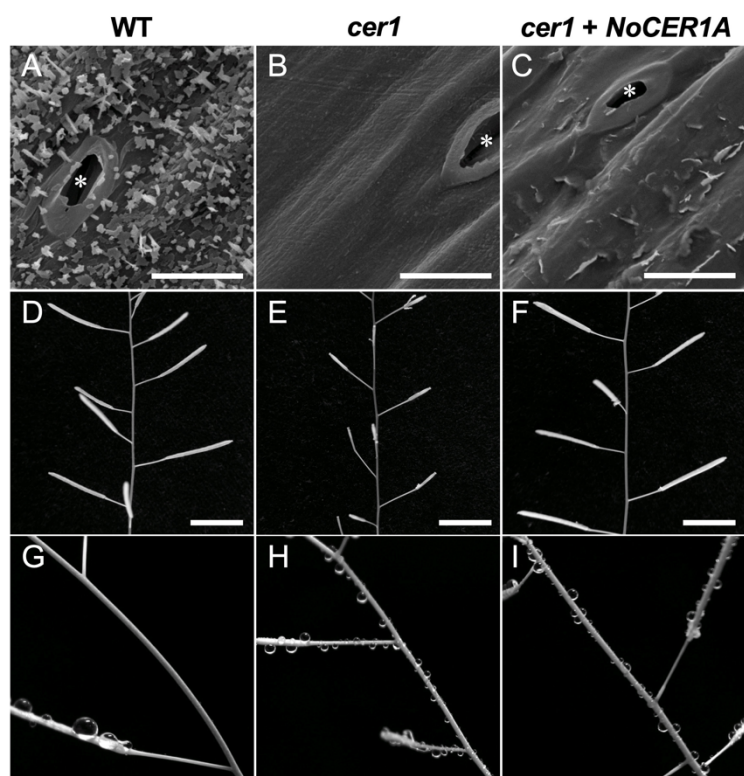


**Figure 7**

#### Epicuticular wax formation and pollen fertility in *NoCER1A*-expressing *cer1*.

(A–C) Scanning electron micrographs of the stem surface in the WT (A), *cer1* (B), and *cer1* containing *ProAt1-NoCER1A* (C). Bar represents 10  $\mu$ m. An asterisk denotes a stoma. (D–F) Fully developed self-pollinated fruits reflecting normal pollen fertility in the WT (D) and *cer1* containing *ProAt1-NoCER1A* (F) in comparison to unfertilized fruits in male-sterile *cer1* (E). The bar represents 10 mm. (G–I) Stems after spraying with water. The WT stem repelled water (G), whereas water droplets adhered to the stems of *cer1* (H), and *cer1* containing *ProAt1-NoCER1A* (I).

water sprayed onto WT plants caused an obvious lotus effect, and no water droplets remained on the stem surface (Fig. 7G). However, after spraying the surface of *NoCERIA*-expressing *cer1* plants and the untransformed *cer1* mutant, we observed that many water droplets adhered to the stem surface (Fig. 7H and I), confirming the hypothesis that the production of wax crystals is important for water shedding. Taken together, these results suggest that *Arabidopsis* acquired the activity to produce C29 alkane exclusively, likely to make self-cleaning more effective.

## DISCUSSION

### Substrate Carbon Chain Length Specificities of NoCER1A and NoCER3A/B

We found that water lilies produce alkanes with shorter carbon chain lengths than those produced by *Arabidopsis*, suggesting that some property of the alkane synthesis enzymes in water lilies directs them to produce shorter alkanes. We isolated full-length CDS clones for an *AtCER1* homolog (*NoCER1A*) and two *AtCER3* homologs (*NoCER3A* and *NoCER3B*) from this species. Complementation experiments in *Arabidopsis cer1* and *cer3* mutants revealed that *NoCER1A* and *NoCER3A/B* are functional counterparts of *AtCER1* and *AtCER3*, respectively. A recently published genome sequence of *N. colorata* revealed that it has two genes that closely resemble *NoCER1A* and two *CER3* genes that corresponded to *NoCER3A* and *NoCER3B*, respectively (Zhang et al. 2020). Hence it is suggested that the shorter alkanes in water lilies are produced by these enzymes. *CER1* and *CER3* are thought to be two separate genes formed by the functional differentiation of a single ancestral gene (Chaudhary et al. 2021; Wang et al. 2019). Phylogenetic analysis of the predicted amino-acid sequences indicated that NoCER1A, together with two *A. trichopoda* proteins, first branched off from other CER1 homologs in angiosperms, which is consistent with the evolutionary position of water lilies. Similar relationships were observed for CER3 proteins.

Introduction of *NoCER1A* restored alkane production in the *Arabidopsis cer6* mutant, in which C28 and longer acyl-CoAs could not be synthesized. Although *AtCER1* was active in the mutant, it could not use C26 or shorter substrates. Similar results were obtained from the experiments using tobacco BY-2 cells, where NoCER1A but not *AtCER1* produced C25 and shorter alkanes in combination with either NoCER3A/B or *AtCER3*. Moreover, NoCER1A effectively produced C29 alkane, when it was introduced into the *cer1* mutant. These results show an unequivocal difference between *AtCER1* and NoCER1A in that the former preferentially produces C29 alkanes, whereas the latter synthesizes C19–C29 alkanes non-selectively. This indicates that *AtCER1* but not NoCER1A shows strict carbon chain length specificity for fatty-aldehyde substrates.

A similar chain length specificity was observed in the activity of midchain alkane hydroxylase, where C29 alkane was effectively converted to C29-15-alcohol and C29-15-ketone, but a negligible amount of C27 and shorter ketones and secondary alcohols were measured even when NoCER1A produced a considerable amount of shorter alkanes (Figs. 3 and 4) (Greer et al. 2007).

### **Predicted 3D Structures of NoCER1A and NoCER3A/B**

Despite the low sequence similarity between NoCER1A and AtCER1, the predicted 3D structures of NoCER1A (A0A7G1GB01) and AtCER1 (F4HVVY0) recorded by the AlphaFold Protein Structure Database closely resembled each other (Supplementary Fig. S13A and B). Each consisted of an N-terminal domain (NTD) comprising His-rich motifs accumulated in a small region coupled with six parallelly aligned helices and a C-terminal domain (CTD) that includes the WAX2 domain. According to homology modeling on the SWISS-MODEL server, the NTD resembles the catalytic domain of yeast sphingolipid  $\alpha$ -hydroxylase, Scs7p (4ZR1), which hydroxylates C-2 of a VLC fatty acid moiety. This domain comprises a His-rich active site and four transmembrane helices to form a lipid-binding channel, which anchors the enzyme to the ER (Supplementary Fig. S13C) (Zhu et al. 2015). The arrangement of CER1 proteins is such that four helices of the six lay on the clustered His residues, and this is coincident with the characteristics of Scs7p (Supplementary Fig. S13D–G). We therefore speculate that the NTD is the catalytic domain of CER1 proteins and the four helices on the His-rich motifs form a lipid-binding channel embedded in the membrane. It has been proposed that a specific amino-acid residue in the lipid-binding channel of Scs7p may help determine the carbon chain length specificity of the substrate (Zhu et al. 2015). Although the amino-acid sequences of the four helices forming the putative lipid-binding channel are not similar in NoCER1A and AtCER1 (Supplementary Fig. S1), 3D structures of this region of the two proteins are nearly identical. Hence, it is difficult to attribute differences in the carbon chain length specificity of these proteins to structural differences between their putative catalytic domains.

Previous studies have elucidated that cyanobacteria employ an acyl-acyl carrier protein reductase (AAR) to convert fatty acyl groups into fatty aldehydes for synthesizing alkanes (Schirmer et al. 2010). Although sequence identity scores between CER3s and AARs were very low (Bernard et al. 2012), a CTD structural model of NoCER3A (A0A7G1G966 in the AlphaFold Database) clearly resembled the cleft region of *Synechococcus elongatus* PCC7942 ARR (SeARR; PDB code 6JZQ) (Supplementary Fig. S14A–C), which has a 3D structure that was determined via X-ray crystallography (Gao et al. 2020). The region was shown to constitute a substrate entrance to the catalytic center and a binding site for NADPH. The catalytic residue, C294, is located at the bottom of the cleft. The overlaid structure revealed that a Cys residue (C577) of NoCER3A was located at the same position as C294 in SeAAR, suggesting that the C577 may be the catalytic residue of NoCER3A (Supplementary Fig. S14A-C). this

hypothesis is consistent with the conservation of the Cys residue in CER3 proteins but not in CER1 proteins (Supplementary Figs. S1, S2, and S14D). The NoCER3A model was almost completely overlaid on the structure of AtCER3 (Q8H1Z0) and NoCER3B (A0A7G1GAG9), which further suggests that the 3D structure is common to all CER3 proteins (Supplementary Fig. S14E–H). Furthermore, the structures of CER1s and CER3s also highly resemble each other (Supplementary Fig. S15).

Despite overall similarity in the structure of CER1 and CER3, the active site is located in different positions in CER1 (at the NTD) and CER3 (at the CTD). This is consistent with the relatively high conservation of the NTD in CER1s and the low conservation of this region in CER3s (and vice versa for the CTD). Recent studies have shown that the ancestral enzyme of CER1 and CER3 was the result of a fusion of two enzymes that differ in both structure and activity (Chaudhary et al. 2021). During subsequent evolution, each may have changed such that only one of the domains became or remained active.

We showed that *N. odorata* CER1 and CER3 respectively rescued Arabidopsis *cer1* and *cer3* mutants, which suggests that *N. odorata* proteins performed their activities in combination with Arabidopsis AtCER1 and AtCER3. Since it has been shown that AtCER1 physically interacts with AtCER3 (Bernard et al. 2012), *N. odorata* and Arabidopsis proteins are thought to be able to form enzymatic complexes. To predict the complex structures of CER1 and CER3, we used AlphaFold2\_advanced. The

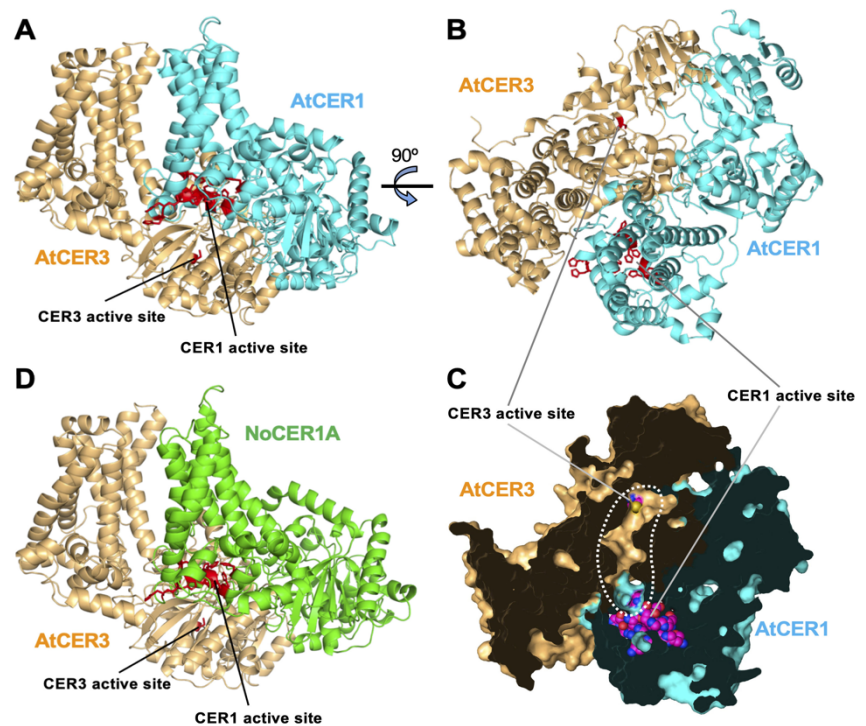


**Figure 8**

**Predicted 3D structures of CER1 and CER3 complexes.**

(A–C) A structure of AtCER1 and AtCER3 complex predicted by AlphaFold2\_advanced. (A) Side view. (B and C) Top view. In (A) and (B), His residues in the tripartite His clusters in AtCER1 and the Cys residue in AtCER3 active site are shown in red. (C) Cutaway view of the putative substrate tunnel (dotted line) connecting the two active sites, of which His and Cys atoms are indicated by spheres. (D) A predicted structure of NoCER1A and AtCER3 complex.

model thus generated showed that AtCER1 and AtCER3 were aligned in the same direction and the NTD of AtCER1 and the CTD of AtCER3 were bound tightly (Fig. 8A, B). Moreover, an internal view of the complex revealed that the putative active sites of CER3 and CER1 were connected by a cavity that extends to the predicted lipid-binding channel of CER1 (Fig. 8C). We therefore speculate that this predicted structure explains the synergistic function of AtCER1 and AtCER3 in alkane production, although no experimental evidence confirming this is currently available. This prediction also suggests that NoCER1A and AtCER3 could form a complex with almost the same structure (Fig. 8D), which is coincident with the cooperative function of NoCER1A and AtCER3 in alkane production. The large substrate-binding cavity may therefore account for the lack of carbon chain length specificity in CER3 proteins.

### **Chain Length Specificity Contributes to Wax Crystal Formation**

In contrast to the C29-preferential alkane production in WT stems, *NoCERIA*-expressing *cer1* plants produced shorter alkanes (i.e., as small as C23), even though the plants possessed functional fatty acid elongases. This indicated that CER1 and CER3 compete with elongase for acyl-CoA substrates in the ER. Incorporation of shorter-chain alkanes into the stem epicuticular wax hindered the crystal formation required for self-cleaning. Similar defects in wax crystal formation have been observed when the amount of C31 alkane exceeded the level of C29 alkane caused by ectopic expression of CER2-LIKE1/CER26 (Haslam et al. 2015; Pascal et al. 2013). Moreover, increased C23 and C25 alkanes in plants overexpressing CER1-LIKE1 also prevented crystallization (Pascal et al. 2019). Therefore, we suggest that the chain length specificity of C29 alkane production is important to prevent competition with elongase for shorter-chain substrates and may have been acquired during the evolution of Arabidopsis. In contrast, *N. odorata* does not require such enzymes, since it does not produce wax crystals on its organ surfaces. It should be noted that pollen fertility of *cer1* completely restored by the expression of *NoCERIA* gene, presumably because no crystal formation is required for the function of pollen coat.

### **Function and Regulation of CER3 in Aldehyde Production**

In plants, there exist two types of acyl-CoA reductases. One type comprises aldehyde-generating enzymes such as CER3. The other type comprises alcohol-generating enzymes that catalyze two-step reactions forming primary alcohols via an aldehyde intermediate, which remains bound to the enzymes

(Doan et al. 2009; Metz et al. 2000). In Arabidopsis, the latter includes FATTY ACYL-COENZYME A REDUCTASE1 (FAR1) to FAR8. It has been shown that FAR3/CER4 produces VLC alcohols in epicuticular waxes (Rowland et al. 2006). FAR1, FAR4, and FAR5 have been found to be involved in suberin formation and FAR2/MS2 are important for sporopollenin formation (Aarts et al. 1997; Dobritsa et al. 2009; Domergue et al. 2010). Even though the *cer3* allele used in our experiments was a null allele, *cer3* mutants produced considerable amounts of alkanes, suggesting that an alternate reductase—i.e., other than AtCER3—provided aldehyde intermediates for alkane production. Since AtCER3 is currently thought to be a unique aldehyde-generating reductase in Arabidopsis, these aldehyde intermediates may be provided by an unidentified enzyme, or possibly by FAR.

While aldehydes accumulated in *cer1*, these levels were much lower than the amount of alkanes present in the WT, even though AtCER3 was active in the mutant (Supplementary Fig. S10). Similarly, the aldehyde levels remained low in *cer6*, in which both AtCER1 and AtCER3 were active, but the former could not work since the substrates with appropriate carbon-chain lengths were never supplied. Taken together, these results suggest that AtCER3 activity was suppressed when AtCER1 was not functional. This may reflect the cooperative function of AtCER1 and AtCER3 in their complex. Alternatively, plants may have a system to suppress the accumulation of toxic aldehydes.

### **Introduction of NoCER1A and one of the CER3 is Sufficient for Alkane Production in Plant Cells**

We found that the introduction of only two genes, *NoCER1A* and any one of the *CER3*s, is sufficient to synthesize C17–C25 alkanes in tobacco BY-2 cells, which do not otherwise produce a detectable amount of alkanes without genetic modification. Our findings therefore show that BY-2 cells can produce VLC acyl-CoA molecules of approximately this range in the ER and that these molecules are available to NoCER1A for alkane production, whereas they are too short for AtCER1. In many plant leaves, C20–C26 VLC fatty acids are synthesized and used to produce sphingolipids and some classes of phospholipids (Bach and Faure 2010). Therefore, it is expected that the expression of NoCER1A and an appropriate CER3 will facilitate the production of VLC alkanes in many plant cells. In addition, our BY-2 expression analysis also revealed slight differences in chain length specificity among CER3 proteins. NoCER3A uses short acyl-CoA substrates (especially C20 and C22) more effectively than others.

The alkane levels produced by transgenic BY-2 cells reached 43–53  $\mu\text{g}$  per g fresh cell weight (or

1.0–1.3 mg per g dry cell weight). Although this yield is 1/500 of the recent record of alkane production in oleaginous yeast *Yarrowia lipolytica* (Bruder et al. 2019; Hu et al. 2019), we provide evidence of alkane production in a heterologous system using water lily alkane-forming enzymes. These BY-2 cells accumulate alkanes presumably in the ER since they lack any specific lipid-storage organelles, but if they develop those organelles such as tapetosome in anther tapetal cells, they may accumulate more alkanes in the cells. Bernard *et al.* (2012) demonstrated that AtCER1 and AtCER3 require VLC fatty acid elongase for alkane production in yeast and that the resulting product was mainly C29 alkane supplemented with a small amount of C27–C31 alkanes. This composition clearly reflected the chain length specificity of AtCER1. Yeast can produce VLC fatty acids up to C26 in length (Welch and Burlingame 1973). Hence, it is expected that the expression of NoCER1 together with an appropriate CER3 can produce VLC alkanes in yeast without requiring the use of VLC fatty acid elongases.

## MATERIALS AND METHODS

### Plant Materials and Growth Conditions

Fragrant water lily (*Nymphaea odorata*) grown in a pond of Nagoya University Museum Botanical Garden was used as the source of pollen-coat lipid and anther RNA. *Arabidopsis* (*Arabidopsis thaliana*) *cer1* (*cer1-1*; SALK\_008544) (Bourdenx et al. 2011), *cer3* (*cer3-9*; GABI\_177D09) (Xu et al. 2019), and *cer6* (*cer6-4*; GABI\_804G08) (established in this paper) mutants were obtained from the *Arabidopsis* Biological Resource Center and Nottingham *Arabidopsis* Stock Centre (Supplementary Fig. S6). All the wild-type and mutant *Arabidopsis* plants used in this study were of Col-0 accession and were grown on vermiculite at 22°C under continuous illumination by fluorescent light. Tobacco (*Nicotiana tabacum*) suspension-cultured cell line BY-2 was maintained in a liquid BY-2 medium (Murashige and Skoog plant salt mixture, 3% sucrose, 200 mg/L KH<sub>2</sub>PO<sub>4</sub>, 100 mg/L *myo*-inositol, 1 mg/L thiamine HCl, 0.2 mg/L 2,4-dichlorophenoxyacetic acid, pH 5.8) with constant rotation (110 rpm) at 25°C under darkness.

### Plant Transformation

Transformation of *Arabidopsis* was carried out as described previously (Ishiguro et al. 2010). To obtain the transformants in *cer3*, *cer1 cer3*, and *cer3 cer6* backgrounds, heterozygotes for *cer3* mutation were used for *Agrobacterium* infection because *cer3* homozygotes were strongly sterile. T1 transformants homozygous for *cer3* mutation were selected by PCR genotyping. For transformation of BY-2 cells, 4 mL of three-day-old BY-2 suspension culture was poured into a 9-cm diameter dish and mixed with 100 µL of fully-grown *Agrobacterium* culture harboring the binary plasmid described below. After static co-cultivation for two days at 25°C, cells were washed with liquid BY-2 medium and scattered on a plate of BY-2 medium solidified with 0.4% gellan gum and 0.1% MgSO<sub>4</sub>·7H<sub>2</sub>O and supplemented with 50 mg/L hygromycin B and 500 mg/L cefotaxime. After cultivation for three to four weeks at 25°C, transformed calli were harvested and used for lipid analysis.

### RNA Extraction

*N. odorata* anthers (200 mg) containing developing tapetal cells were harvested, frozen in liquid nitrogen, and powdered together with 1 mL TRIzol Reagent (Thermo-Fisher Scientific) using a frozen

mortar and pestle. The powder was transferred to pre-heated (70°C) mortar and further ground with pre-heated 1 mL TRIzol Reagent. After adding 400 µL chloroform, crude RNA was collected from the aqueous phase by isopropanol precipitation. The RNA was purified using an RNeasy plant mini kit (Qiagen). Arabidopsis RNA in flower bud clusters was both extracted and purified using an RNeasy plant mini kit.

### **Reverse Transcription and Degenerate PCR**

*N. odorata* anther RNA (0.5 µg) was reverse transcribed with ReverTra Ace qPCR Master Mix with gDNA Remover (Toyobo). The resulting first strand cDNA was used as a template for PCR amplification with degenerate *CER1* and *CER3* primers (Supplementary Table S3) using PrimeSTAR HS DNA polymerase (Takara Bio). PCR products were cloned in the *Sma* I site of pUC119, and eight independently obtained clones were sequenced.

### **NGS Analysis**

A cDNA library was constructed from 0.5 µg anther RNA using a TruSeq RNA Sample Preparation Kit (Illumina) and was used for paired end sequencing for 60 cycles by Illumina Genome Analyzer IIX. Sequence reads were *de novo* assembled into contigs by Trinity software (Grabherr et al. 2011).

### **Preparation of Full Length CDS Clones**

All the primers used for cloning and plasmid construction are listed in Supplementary Table S3. Full-length CDS for *NoCER1A*, *NoCER3A*, and *NoCER3B* were amplified by PCR from water lily anther cDNA as described above. Primers were designed according to the NGS data. The CDS fragments were cloned in the *Sma* I site of pUC119. Resulting plasmids were designated as pUC-NyCER1A, pUC-NyCER3A, and pUC-NyCER3B. Full-length CDS fragments of *AtCER1* and *AtCER3* were prepared by RT-PCR from Arabidopsis young flower bud RNA and cloned into pDONR201 by Gateway BP reaction (Thermo-Fisher Scientific). They were named pDONR-AtCER1 and pDONR-AtCER3.

### **Phylogenetic Analysis**

Maximum-likelihood phylogenetic trees were constructed using MEGA11 software with 1000 bootstrap replicates (Tamura et al. 2021). The sequences used to make the trees are listed in Supplementary Table

S2.

### **Construction of Plasmids for *CER1* and *CER3* Gene Expression**

All plant transformation plasmids for *CER* gene expression were prepared by way of the Gateway recycling cloning system (Kimura et al. 2013). Details are described in Supplementary Methods.

### **Lipid Extraction**

Anthers harvested from fully opened flowers were immersed in water in a microcentrifuge tube and vortexed vigorously. Suspended pollen grains were collected by centrifugation, and their surface lipid (pollen coat) was extracted with a small volume of chloroform (300  $\mu$ L). After evaporation of solvent by N<sub>2</sub> gas flow, the deposited pollen coat was dissolved in hexane and served for GC-MS analysis.

To extract stem cuticular wax, a cut piece of the basal part (3 cm in length) of the lateral shoot branched from the main shoot was harvested into a microcentrifuge tube. A small volume of chloroform (200  $\mu$ L) was added into the tube, and lipid was extracted with gentle mixing for 30 s. After evaporation of solvent by N<sub>2</sub> gas flow, the precipitated lipid was dissolved in hexane and served for GC-MS analysis. To quantify the absolute alkane levels, 300 ng of C15 alkane was added to the samples at chloroform extraction as an internal standard.

A part (10–30 mg) of BY-2 calli grown on the solidified medium was harvested into a microcentrifuge tube. A small volume (300  $\mu$ L) of chloroform/methanol (1/1) was added to the cells, and vigorous vortexing was performed for 1 min to extract lipids. After centrifugation to remove cells, the extract was dried with N<sub>2</sub> gas flow and dissolved in hexane for GC-MS analysis. To quantify the absolute alkane levels, 300 ng of C15 alkane was added to the samples at chloroform/methanol extraction as an internal standard.

### **GC-MS Analysis**

Lipids were analyzed by a mass spectrometer, JMS-K9 (JEOL), equipped with a DB-1 column (30 m  $\times$  0.25 mm ID  $\times$  0.25  $\mu$ m film) (Agilent Technologies) under the following parameters: He gas flow, 1.5 mL/min; oven temperature, 50–200°C (50°C/min) and then 200–300°C (5°C/min). Separated samples were ionized by electron ionization at 70 eV, and a m/z range of 50–500 was detected. We used  $\beta$ -amyrin and palmitic acid as endogenous internal standards for the quantification of alkanes in

Arabidopsis stem waxes and in BY-2 cells, respectively. For absolute quantification of wax components, amounts were normalized by the levels of exogenously added C15 alkane and were corrected by relative response factors determined in our condition (0.19 for primary alcohols and 1.0 for aldehydes). For statistical analysis, we used the non-parametric U-test, Steel's test, and Steel–Dwass test for alkane quantification in T1 plants because some data did not follow a normal distribution. For the data of T2 plants and BY-2 cells, we used the parametric Tukey's test or Tukey–Kramer test.

### **Scanning Electron Microscopy**

A cut piece of the basal part of lateral stems that branched off from the main shoot was attached on an aluminum stab with double-sided adhesive tape and coated with Au in an ion sputter (MSP-1S, Vacuum Device). The specimen was observed by a scanning electron microscope (S-2600N, Hitachi) at an accelerating voltage of 10 kV in high vacuum mode.

### **Prediction of protein structures**

The modeling tool in SWISS-MODEL server (<https://swissmodel.expasy.org/>) was used to find a template of CER1 NTD. PDB files of proteins were obtained from PDB database (<https://www.rcsb.org/>) and AlphaFold Protein Structure Database (<https://alphafold.ebi.ac.uk/>) and visualized by PyMOL software (<https://pymol.org/>). Structures of CER1 and CER3 complex were modeled by AlphaFold2\_advanced software ([https://colab.research.google.com/github/sokrypton/ColabFold/blob/main/beta/AlphaFold2\\_advanced.ipynb](https://colab.research.google.com/github/sokrypton/ColabFold/blob/main/beta/AlphaFold2_advanced.ipynb)).

### **Supplementary Data**

Supplementary data are available at *PCP* online.

### **Data Availability**

Nucleotide sequences of CDS clones: NoCER1A (LC422236), NoCER3A (LC422237), NoCER3B (LC422238). FASTQ file of the NGS reads of *N. odorata* anther RNA: DRA007258.

## **Funding**

This work was supported by KAKENHI grants from Japan Society for the Promotion of Science and Ministry of Education, Culture, Sports, Science and Technology [JP18H00322 and JP19H00302 to HK; JP18K06281, JP19H05362 and JP21H00365 to SI], ALCA program from Japan Science and Technology Agency [to SI and KT], and a collaborative research fund from Toyota Central R&D Laboratories, Inc. [to SI]. The NGS analysis of *N. odorata* anther transcripts was supported by JST ERATO project [JPMJER1004 to TH].

## **Disclosures**

The authors have no conflicts of interest to declare.

## **Acknowledgments**

We thank Natsuko Yoshino, Sachiko Nishida, and Nagoya University Museum Botanical Garden for providing *N. odorata* samples; Higashiyama Zoo and Botanical Gardens for providing other *Nymphaea* samples; Sumiyo Suzuki, Fujio Suzuki, and Miyoko Kojima for collecting pollen samples from various flowers; the Arabidopsis Biological Resource Center and Nottingham Arabidopsis Stock Centre for providing Arabidopsis seed; Norihiro Mitsukawa, Nobuhiko Muramoto, Risa Nagura, Kunihiro Ohta, Kazuto Kugo, Takahiro Nakamura, Kenichiro Maeo, Shin-ichi Maeda, Yoichi Nakanishi, and Kenzo Nakamura for helpful discussion; and Rie Seizako for some preliminary analysis.

## **Author contributions**

H.K. performed the most experiments; K.Y. cloned the genes; T.S. performed the NGS analysis; Y.H. generated the transgenic plants; T.N. performed the protein modeling analysis; K.T. and S.K. performed the expression analysis; T.H. supervised the NGS analysis; H.K. and S.I. designed the experiments and analyzed the data; H.K. wrote a draft of the manuscript; SI complete the manuscript with contribution of all the authors.

## References

- Aarts, M.G., Hodge, R., Kalantidis, K., Florack, D., Wilson, Z.A., Mulligan, B.J., et al. (1997) The Arabidopsis MALE STERILITY 2 protein shares similarity with reductases in elongation/condensation complexes. *Plant J.* 12: 615-623.
- Aarts, M.G., Keijzer, C.J., Stiekema, W.J. and Pereira, A. (1995) Molecular characterization of the CER1 gene of Arabidopsis involved in epicuticular wax biosynthesis and pollen fertility. *Plant Cell* 7: 2115-2127.
- Ariizumi, T., Hatakeyama, K., Hinata, K., Sato, S., Kato, T., Tabata, S., et al. (2003) A novel male-sterile mutant of Arabidopsis thaliana, faceless pollen-1, produces pollen with a smooth surface and an acetolysis-sensitive exine. *Plant Mol. Biol.* 53: 107-116.
- Bach, L. and Faure, J.D. (2010) Role of very-long-chain fatty acids in plant development, when chain length does matter. *C R Biol* 333: 361-370.
- Bernard, A., Domergue, F., Pascal, S., Jetter, R., Renne, C., Faure, J.D., et al. (2012) Reconstitution of plant alkane biosynthesis in yeast demonstrates that Arabidopsis ECERIFERUM1 and ECERIFERUM3 are core components of a very-long-chain alkane synthesis complex. *Plant Cell* 24: 3106-3118.
- Bernard, A. and Joubès, J. (2013) Arabidopsis cuticular waxes: advances in synthesis, export and regulation. *Prog Lipid Res* 52: 110-129.
- Bertoli, A., Fambrini, M., Doveri, S., Leonardi, M., Pugliesi, C. and Pistelli, L. (2011) Pollen aroma fingerprint of two sunflower (*Helianthus annuus* L.) genotypes characterized by different pollen colors. *Chem. Biodivers.* 8: 1766-1775.
- Bourdenx, B., Bernard, A., Domergue, F., Pascal, S., Leger, A., Roby, D., et al. (2011) Overexpression of Arabidopsis ECERIFERUM1 promotes wax very-long-chain alkane biosynthesis and influences plant response to biotic and abiotic stresses. *Plant Physiol.* 156: 29-45.
- Bruder, S., Moldenhauer, E.J., Lemke, R.D., Ledesma-Amaro, R. and Kabisch, J. (2019) Drop-in biofuel production using fatty acid photodecarboxylase from *Chlorella variabilis* in the oleaginous yeast *Yarrowia lipolytica*. *Biotechnol Biofuels* 12: 202.
- Buschhaus, C. and Jetter, R. (2012) Composition and physiological function of the wax layers coating Arabidopsis leaves: beta-amyrin negatively affects the intracuticular water barrier. *Plant Physiol.*

- 160: 1120-1129.
- Busta, L. and Jetter, R. (2017) Structure and biosynthesis of branched wax compounds on wild type and wax biosynthesis mutants of *Arabidopsis thaliana*. *Plant Cell Physiol.*
- Chaudhary, K., Geeta, R. and Panjabi, P. (2021) Origin and diversification of ECERIFERUM1 (CER1) and ECERIFERUM3 (CER3) genes in land plants and phylogenetic evidence that the ancestral CER1/3 gene resulted from the fusion of pre-existing domains. *Mol Phylogenet Evol* 159: 107101.
- Cheesbrough, T.M. and Kolattukudy, P.E. (1984) Alkane biosynthesis by decarbonylation of aldehydes catalyzed by a particulate preparation from *Pisum sativum*. *Proc Natl Acad Sci U S A* 81: 6613-6617.
- Chen, X., Goodwin, S.M., Boroff, V.L., Liu, X. and Jenks, M.A. (2003) Cloning and characterization of the WAX2 gene of *Arabidopsis* involved in cuticle membrane and wax production. *Plant Cell* 15: 1170-1185.
- Choi, Y.J. and Lee, S.Y. (2013) Microbial production of short-chain alkanes. *Nature* 502: 571-+.
- Doan, T.T., Carlsson, A.S., Hamberg, M., Bulow, L., Stymne, S. and Olsson, P. (2009) Functional expression of five *Arabidopsis* fatty acyl-CoA reductase genes in *Escherichia coli*. *J. Plant Physiol.* 166: 787-796.
- Dobritsa, A.A., Shrestha, J., Morant, M., Pinot, F., Matsuno, M., Swanson, R., et al. (2009) CYP704B1 is a long-chain fatty acid omega-hydroxylase essential for sporopollenin synthesis in pollen of *Arabidopsis*. *Plant Physiol.* 151: 574-589.
- Domergue, F., Vishwanath, S.J., Joubes, J., Ono, J., Lee, J.A., Bourdon, M., et al. (2010) Three *Arabidopsis* fatty acyl-coenzyme A reductases, FAR1, FAR4, and FAR5, generate primary fatty alcohols associated with suberin deposition. *Plant Physiol.* 153: 1539-1554.
- Fich, E.A., Segerson, N.A. and Rose, J.K. (2016) The Plant Polyester Cutin: Biosynthesis, Structure, and Biological Roles. *Annu. Rev. Plant Biol.* 67: 207-233.
- Fiebig, A., Mayfield, J.A., Miley, N.L., Chau, S., Fischer, R.L. and Preuss, D. (2000) Alterations in CER6, a gene identical to CUT1, differentially affect long-chain lipid content on the surface of pollen and stems. *Plant Cell* 12: 2001-2008.
- Foo, J.L., Susanto, A.V., Keasling, J.D., Leong, S.S. and Chang, M.W. (2017) Whole-cell biocatalytic and de novo production of alkanes from free fatty acids in *Saccharomyces cerevisiae*. *Biotechnol. Bioeng.* 114: 232-237.
- Gao, Y., Zhang, H., Fan, M., Jia, C., Shi, L., Pan, X., et al. (2020) Structural insights into catalytic

- mechanism and product delivery of cyanobacterial acyl-acyl carrier protein reductase. *Nat Commun* 11: 1525.
- Garay, L.A., Boundy-Mills, K.L. and German, J.B. (2014) Accumulation of High-Value Lipids in Single-Cell Microorganisms: A Mechanistic Approach and Future Perspectives. *J. Agric. Food Chem.* 62: 2709-2727.
- Goodwin, S.M., Rashotte, A.M., Rahman, M., Feldmann, K.A. and Jenks, M.A. (2005) Wax constituents on the inflorescence stems of double eceriferum mutants in Arabidopsis reveal complex gene interactions. *Phytochemistry* 66: 771-780.
- Grabherr, M.G., Haas, B.J., Yassour, M., Levin, J.Z., Thompson, D.A., Amit, I., et al. (2011) Full-length transcriptome assembly from RNA-Seq data without a reference genome. *Nat. Biotechnol.* 29: 644-652.
- Greer, S., Wen, M., Bird, D., Wu, X., Samuels, L., Kunst, L., et al. (2007) The cytochrome P450 enzyme CYP96A15 is the midchain alkane hydroxylase responsible for formation of secondary alcohols and ketones in stem cuticular wax of Arabidopsis. *Plant Physiol.* 145: 653-667.
- Haslam, T.M., Haslam, R., Thoraval, D., Pascal, S., Delude, C., Domergue, F., et al. (2015) ECERIFERUM2-LIKE Proteins Have Unique Biochemical and Physiological Functions in Very-Long-Chain Fatty Acid Elongation. *Plant Physiol.* 167: 682-+.
- Haslam, T.M. and Kunst, L. (2013) Extending the story of very-long-chain fatty acid elongation. *Plant Sci.* 210: 93-107.
- Haslam, T.M., Manas-Fernandez, A., Zhao, L.F. and Kunst, L. (2012) Arabidopsis ECERIFERUM2 Is a Component of the Fatty Acid Elongation Machinery Required for Fatty Acid Extension to Exceptional Lengths. *Plant Physiol.* 160: 1164-1174.
- Henry, S.A., Kohlwein, S.D. and Carman, G.M. (2012) Metabolism and Regulation of Glycerolipids in the Yeast *Saccharomyces cerevisiae*. *Genetics* 190: 317-349.
- Hu, Y., Zhu, Z., Nielsen, J. and Siewers, V. (2019) Engineering *Saccharomyces cerevisiae* cells for production of fatty acid-derived biofuels and chemicals. *Open Biol* 9: 190049.
- Hülkamp, M., Kopczak, S.D., Horejsi, T.F., Kihl, B.K. and Pruitt, R.E. (1995) Identification of genes required for pollen-stigma recognition in *Arabidopsis thaliana*. *Plant J.* 8: 703-714.
- Ishiguro, S., Nishimori, Y., Yamada, M., Saito, H., Suzuki, T., Nakagawa, T., et al. (2010) The Arabidopsis *FLAKY POLLENI* gene encodes a 3-hydroxy-3-methylglutaryl-coenzyme A synthase

- required for development of tapetum-specific organelles and fertility of pollen grains. *Plant Cell Physiol.* 51: 896-911.
- Islam, M.A., Du, H., Ning, J., Ye, H. and Xiong, L. (2009) Characterization of Glossy1-homologous genes in rice involved in leaf wax accumulation and drought resistance. *Plant Mol. Biol.* 70: 443-456.
- Jenks, M.A., Tuttle, H.A., Eigenbrode, S.D. and Feldmann, K.A. (1995) Leaf Epicuticular Waxes of the Eceriferum Mutants in Arabidopsis. *Plant Physiol.* 108: 369-377.
- Jenks, M.A., Tuttle, H.A. and Feldmann, K.A. (1996) Changes in epicuticular waxes on wildtype and Eceriferum mutants in Arabidopsis during development. *Phytochemistry* 42: 29-34.
- Jung, K.H., Han, M.J., Lee, D.Y., Lee, Y.S., Schreiber, L., Franke, R., et al. (2006) Wax-deficient anther1 is involved in cuticle and wax production in rice anther walls and is required for pollen development. *Plant Cell* 18: 3015-3032.
- Kang, M.K., Zhou, Y.J., Buijs, N.A. and Nielsen, J. (2017) Functional screening of aldehyde decarbonylases for long-chain alkane production by *Saccharomyces cerevisiae*. *Microb Cell Fact* 16: 74.
- Kimura, T., Nakao, A., Murata, S., Kobayashi, Y., Tanaka, Y., Shibahara, K., et al. (2013) Development of the gateway recycling cloning system for multiple linking of expression cassettes in a defined order, and direction on gateway compatible binary vectors. *Biosci Biotechnol Biochem* 77: 430-434.
- Koornneef, M., Hanhart, C.J. and Thiel, F. (1989) A Genetic and Phenotypic Description of Eceriferum (Cer) Mutants in Arabidopsis-Thaliana. *J. Hered.* 80: 118-122.
- Kurata, T., Kawabata-Awai, C., Sakuradani, E., Shimizu, S., Okada, K. and Wada, T. (2003) The YORE-YORE gene regulates multiple aspects of epidermal cell differentiation in Arabidopsis. *Plant J.* 36: 55-66.
- Lai, C., Kunst, L. and Jetter, R. (2007) Composition of alkyl esters in the cuticular wax on inflorescence stems of Arabidopsis thaliana cer mutants. *Plant J.* 50: 189-196.
- Lee, S.B. and Suh, M.C. (2015) Advances in the understanding of cuticular waxes in Arabidopsis thaliana and crop species. *Plant Cell Rep.* 34: 557-572.
- Li, J., Ma, Y., Liu, N., Eser, B.E., Guo, Z., Jensen, P.R., et al. (2020) Synthesis of high-titer alka(e)nes in *Yarrowia lipolytica* is enabled by a discovered mechanism. *Nat Commun* 11: 6198.
- Lü, S.Y., Song, T., Kosma, D.K., Parsons, E.P., Rowland, O. and Jenks, M.A. (2009) Arabidopsis CER8

- encodes LONG-CHAIN ACYL-COA SYNTHETASE 1 (LACS1) that has overlapping functions with LACS2 in plant wax and cutin synthesis. *Plant J.* 59: 553-564.
- Mao, B., Cheng, Z., Lei, C., Xu, F., Gao, S., Ren, Y., et al. (2012) Wax crystal-sparse leaf2, a rice homologue of WAX2/GL1, is involved in synthesis of leaf cuticular wax. *Planta* 235: 39-52.
- Metz, J.G., Pollard, M.R., Anderson, L., Hayes, T.R. and Lassner, M.W. (2000) Purification of a jojoba embryo fatty acyl-coenzyme A reductase and expression of its cDNA in high erucic acid rapeseed. *Plant Physiol.* 122: 635-644.
- Millar, A.A., Clemens, S., Zachgo, S., Giblin, E.M., Taylor, D.C. and Kunst, L. (1999) CUT1, an Arabidopsis gene required for cuticular wax biosynthesis and pollen fertility, encodes a very-long-chain fatty acid condensing enzyme. *Plant Cell* 11: 825-838.
- Monteiro, R.R.C., da Silva, S.S.O., Cavalcante, C.L., Jr., de Luna, F.M.T., Bolivar, J.M., Vieira, R.S., et al. (2022) Biosynthesis of alkanes/alkenes from fatty acids or derivatives (triacylglycerols or fatty aldehydes). *Biotechnol. Adv.* 61: 108045.
- Mukherjee, A., Sarkar, N. and Barik, A. (2013) Alkanes in flower surface waxes of *Momordica cochinchinensis* influence attraction to *Aulacophora foveicollis* Lucas (Coleoptera: Chrysomelidae). *Neotrop. Entomol.* 42: 366-371.
- Neinhuis, C., Wolter, M. and Barthlott, W. (1992) Epicuticular Wax of Brassica-Oleracea - Changes of Microstructure and Ability to Be Contaminated of Leaf Surfaces after Application of Triton X-100. *Zeitschrift Fur Pflanzenkrankheiten Und Pflanzenschutz-Journal of Plant Diseases and Protection* 99: 542-549.
- Ni, E., Zhou, L., Li, J., Jiang, D., Wang, Z., Zheng, S., et al. (2018) OsCER1 Plays a Pivotal Role in Very-Long-Chain Alkane Biosynthesis and Affects Plastid Development and Programmed Cell Death of Tapetum in Rice (*Oryza sativa* L.). *Front Plant Sci* 9: 1217.
- Pascal, S., Bernard, A., Deslous, P., Gronnier, J., Fournier-Goss, A., Domergue, F., et al. (2019) Arabidopsis CER1-LIKE1 Functions in a Cuticular Very-Long-Chain Alkane-Forming Complex. *Plant Physiol.* 179: 415-432.
- Pascal, S., Bernard, A., Sorel, M., Pervent, M., Vile, D., Haslam, R.P., et al. (2013) The Arabidopsis cer26 mutant, like the cer2 mutant, is specifically affected in the very long chain fatty acid elongation process. *Plant J.* 73: 733-746.
- Pellicer, J., Kelly, L.J., Magdalena, C. and Leitch, I.J. (2013) Insights into the dynamics of genome size

- and chromosome evolution in the early diverging angiosperm lineage Nymphaeales (water lilies). *Genome* 56: 437-449.
- Preuss, D., Lemieux, B., Yen, G. and Davis, R.W. (1993) A conditional sterile mutation eliminates surface components from *Arabidopsis* pollen and disrupts cell signaling during fertilization. *Genes Dev.* 7: 974-985.
- Qin, B.X., Tang, D., Huang, J., Li, M., Wu, X.R., Lu, L.L., et al. (2011) Rice OsGL1-1 is involved in leaf cuticular wax and cuticle membrane. *Mol Plant* 4: 985-995.
- Qiu, Y., Tittiger, C., Wicker-Thomas, C., Le Goff, G., Young, S., Wajnberg, E., et al. (2012) An insect-specific P450 oxidative decarbonylase for cuticular hydrocarbon biosynthesis. *Proc Natl Acad Sci U S A* 109: 14858-14863.
- Rowland, O., Lee, R., Franke, R., Schreiber, L. and Kunst, L. (2007) The CER3 wax biosynthetic gene from *Arabidopsis thaliana* is allelic to WAX2/YRE/FLP1. *FEBS Lett.* 581: 3538-3544.
- Rowland, O., Zheng, H.Q., Hepworth, S.R., Lam, P., Jetter, R. and Kunst, L. (2006) CER4 encodes an alcohol-forming fatty acyl-coenzyme A reductase involved in cuticular wax production in *Arabidopsis*. *Plant Physiol.* 142: 866-877.
- Schirmer, A., Rude, M.A., Li, X., Popova, E. and del Cardayre, S.B. (2010) Microbial biosynthesis of alkanes. *Science* 329: 559-562.
- Tamura, K., Stecher, G. and Kumar, S. (2021) MEGA11: Molecular Evolutionary Genetics Analysis Version 11. *Mol. Biol. Evol.* 38: 3022-3027.
- Tsai, W.T. (2019) An overview of health hazards of volatile organic compounds regulated as indoor air pollutants. *Rev Environ Health* 34: 81-89.
- Wang, H., Ni, X. and Harris-Shultz, K. (2019) Molecular evolution of the plant ECERIFERUM1 and ECERIFERUM3 genes involved in aliphatic hydrocarbon production. *Comput. Biol. Chem.* 80: 1-9.
- Wang, X., Guan, Y., Zhang, D., Dong, X., Tian, L. and Qu, L.Q. (2017) A beta-Ketoacyl-CoA Synthase Is Involved in Rice Leaf Cuticular Wax Synthesis and Requires a CER2-LIKE Protein as a Cofactor. *Plant Physiol.* 173: 944-955.
- Warui, D.M., Li, N., Norgaard, H., Krebs, C., Bollinger, J.M. and Booker, S.J. (2011) Detection of Formate, Rather than Carbon Monoxide, As the Stoichiometric Coproduct in Conversion of Fatty Aldehydes to Alkanes by a Cyanobacterial Aldehyde Decarbonylase. *J. Am. Chem. Soc.* 133: 3316-3319.

- Welch, J.W. and Burlingame, A.L. (1973) Very Long-Chain Fatty-Acids in Yeast. *J. Bacteriol.* 115: 464-466.
- Xu, F., Li, X., Yang, Z. and Zhang, S. (2019) Arabidopsis ECERIFERUM3 (CER3) Plays a Critical Role in Maintaining Hydration for Pollen-Stigma Recognition during Fertilization. *Biorxiv*.
- Yunus, I.S., Wichmann, J., Wordenweber, R., Lauersen, K.J., Kruse, O. and Jones, P.R. (2018) Synthetic metabolic pathways for photobiological conversion of CO<sub>2</sub> into hydrocarbon fuel. *Metab. Eng.* 49: 201-211.
- Zhang, L., Chen, F., Zhang, X., Li, Z., Zhao, Y., Lohaus, R., et al. (2020) The water lily genome and the early evolution of flowering plants. *Nature* 577: 79-84.
- Zhou, L., Ni, E., Yang, J., Zhou, H., Liang, H., Li, J., et al. (2013) Rice OsGL1-6 is involved in leaf cuticular wax accumulation and drought resistance. *PLoS One* 8: e65139.
- Zhou, X., Li, L., Xiang, J., Gao, G., Xu, F., Liu, A., et al. (2015) OsGL1-3 is involved in cuticular wax biosynthesis and tolerance to water deficit in rice. *PLoS One* 10: e116676.
- Zhu, G., Koszelak-Rosenblum, M., Connelly, S.M., Dumont, M.E. and Malkowski, M.G. (2015) The Crystal Structure of an Integral Membrane Fatty Acid alpha-Hydroxylase. *J. Biol. Chem.* 290: 29820-29833.

## LEGENDS TO FIGURES

### Figure 1

Total ion current chromatogram of the GC-MS analysis of pollen coat lipids.

(A) *N. odorata*. (B) Arabidopsis. Arrowheads indicate the peaks of aliphatic compounds of the indicated carbon chain length. Red, alkanes (numbers only); purple, fatty acids (P, palmitic acid; S, stearic acid); gray, ketones (labeled by 'k'); green, secondary alcohols (labeled by 's'). Alkanes labeled by 'm' are branched 2-methylalkanes. The peaks of 2-methyltriacontane and nonacosan-15-one are overlapping. a to d in panel (A) are terpenoids (a, phytol; b, geranylinalool; c, squalene; d,  $\beta$ -sitosterol). Asterisks in (B) are artifacts due to column contamination. RT, retention time. The vertical axis shows the relative intensity when the maximum peak is set as 1.0.

### Figure 2

Structural relationships among CER1 and CER3 proteins in *N. odorata* and representative angiosperms. Maximum likelihood phylogenetic tree of NoCER1A, NoCER3A, NoCER3B, and their homologous proteins in tomato, alfalfa, Arabidopsis, rice, and *A. trichopoda*. A predicted common homolog in *O. tauri* is added as an outgroup. Proteins are color coded according to species. Bootstrap support values from 1000 replicates are indicated. The bar represents 0.2 substitutions per site.

### Figure 3

Restored alkane production in the stems of Arabidopsis *cer1 cer3* plants expressing both *NoCER1A* and *NoCER3A/B*.

(A–E) Total ion current chromatogram of the GC-MS analysis. Typical results of the WT (A), *cer1 cer3* double mutants (B), *cer1 cer3* containing *ProAt1-NoCER1A* and *ProAt3i-NoCER3A* (C), *cer1 cer3* containing *ProAt1-NoCER1A* and *ProAt3i-NoCER3B* (D), and *cer1 cer3* containing *ProAt1-AtCER1* and *ProAt3i-AtCER3* (E) are shown. The vertical axis shows the relative intensity when the maximum peak is set as 1.0. Colored arrowheads indicate the peaks of compounds of the indicated carbon chain length. Red, alkanes (numbers only); black, aldehydes (labeled by 'a'); gray, ketones (labeled by 'k'); green, secondary alcohols (labeled by 's'); blue, primary alcohols (labeled by 'o'). A,  $\beta$ -amyrin, an internal standard for quantification. Peaks with no labels are unidentified compounds. (F) Comparison

of alkane levels shown as relative values compared to the average of the WT. Bars represent individual WT, *cer1 cer3*, and independent T1 transformant plants. The ranges of carbon chain lengths are shown in different colors. Dark green values represent the average ratios of C28 and shorter alkanes against total alkanes. Asterisks indicate statistically significant differences of total alkane amount from *cer1 cer3* (black) and of shorter alkane ratio from WT (dark green), respectively (Steel's test,  $P < 0.05$ ). nd, not determined due to no detection of alkanes.

#### Figure 4

Contribution of NoCER1A and NoCER3A/B to the chain length specificity of alkanes produced in Arabidopsis stems.

(A–E) Total ion current chromatogram of GC-MS analysis. Typical results of *cer1* (A), *cer1* containing *ProAt1-NoCER1A* (B), *cer3* (C), *cer3* containing *ProAt1-NoCER3A* (D), and *cer3* containing *ProAt1-NoCER3B* (E) are shown. (F) Quantification of alkane levels. Statistically significant differences of shorter alkane ratio from WT (dark green \*, Steel's test,  $P < 0.05$ ), of total alkane level from *cer1* (#, U-test,  $P < 0.05$ ), and of total alkane levels from *cer3* (black \*, Steel's test,  $P < 0.05$ ) are indicated. Other details are explained in Figure 3 legend.

#### Figure 5

Production of short VLC alkanes in *cer6* and *cer3 cer6* mutants expressing *N. odorata* genes.

(A–F) Total ion current chromatogram of GC-MS analysis. Typical results of *cer6* (A), *cer6* containing *ProAt1-NoCER1A* (B), *cer6* containing *ProAt1-AtCER1* and *ProAt3-AtCER3* (C), *cer3 cer6* (D), *cer3 cer6* containing *ProAt1-NoCER1A* and *ProAt1-NoCER3A* (E), and *cer3 cer6* containing *ProAt1-NoCER1A* and *ProAt1-NoCER3B* (F) are shown. (G) Quantification of alkane levels. Statistically significant differences of shorter alkane ratio from WT are indicated (dark green \*, Steel's test,  $P < 0.05$ ). Relationships of total alkane levels with a statistically significant difference are shown (Steel's test [\*] and Steel-Dwass test [#],  $P < 0.05$ ). Other details are explained in Figure 3 legend.

#### Figure 6

Alkane production in tobacco BY-2 cells expressing *NoCER1A* and various *CER3* genes.

(A–F) Total ion current chromatogram of the GC-MS analysis. Typical results of a non-transformed BY-

2 callus (A) and BY-2 calli containing *Pro35S-NoCER1A* alone (B), *Pro35S-NoCER1A* and *Pro35S-NoCER3A* (C), *Pro35S-NoCER1A* and *Pro35S-NoCER3B* (D), *Pro35S-AtCER1* and *Pro35S-AtCER3* (E), and *Pro35S-NoCER1A* and *Pro35S-AtCER3* (F) are shown. The vertical axis shows the relative intensity when the maximum peak is set as 1.0. Alkane peaks are labeled with red numbers indicating carbon chain length. P, palmitic acid; L, linoleic acid; O, oleic acid; S, stearic acid. (G) Total alkane levels in six independently obtained transformants expressing indicated genes. Ranges of carbon chain lengths are shown in different colors. Levels are shown in arbitrary units. Significant differences determined by Tukey's test ( $P < 0.05$ ) are indicated by letters above the bars.

### Figure 7

Epicuticular wax formation and pollen fertility in *NoCER1A*-expressing *cer1*.

(A–C) Scanning electron micrographs of the stem surface in the WT (A), *cer1* (B), and *cer1* containing *ProAt1-NoCER1A* (C). Bar represents 10  $\mu$ m. An asterisk denotes a stoma. (D–F) Fully developed self-pollinated fruits reflecting normal pollen fertility in the WT (D) and *cer1* containing *ProAt1-NoCER1A* (F) in comparison to unfertilized fruits in male-sterile *cer1* (E). The bar represents 10 mm. (G–I) Stems after spraying with water. The WT stem repelled water (G), whereas water droplets adhered to the stems of *cer1* (H), and *cer1* containing *ProAt1-NoCER1A* (I).

### Figure 8

Predicted 3D structures of CER1 and CER3 complexes.

(A–C) A structure of AtCER1 and AtCER3 complex predicted by AlphaFold2\_advanced. (A) Side view. (B and C) Top view. In (A) and (B), His residues in the tripartite His clusters in AtCER1 and the Cys residue in AtCER3 active site are shown in red. (C) Cutaway view of the putative substrate tunnel (dotted line) connecting the two active sites, of which His and Cys atoms are indicated by spheres. (D) A predicted structure of NoCER1A and AtCER3 complex.